NOVEL CATIONIC LIPOPLEXES IN GENE DELIVERY

Maria Laakko
University of Helsinki
Faculty of Pharmacy
Division of Pharmaceutical Biosciences
May 2017

HELSINGIN YLIOPISTO
HELSINGFORS UNIVERSITET
UNIVERSITY OF HELSINKI

Tiedekunta/Osasto Fakultet/Sektion – Faculty	Osasto/Sektion– Department	
Faculty of Pharmacy	Division of Pharmaceutical Biosciences	
Tekijä/Författare – Author		
Maria Laakko		
Työn nimi / Arbetets titel – Title		
Novel cationic lipoplexes in gene delivery		
Oppiaine /Läroämne – Subject		
Biopharmacy		
Työn laji/Arbetets art – Level	Aika/Datum – Month and year	Sivumäärä/ Sidoantal – Number of pages
Master's thesis	May 2017	60 + 1

Tiivistelmä/Referat – Abstract

Gene therapy is the therapeutic delivery of nucleic acid sequences into cells, where they can replace a gene that is missing, mutated or poorly expressed. It is a potential treatment to cure e.g. genetic diseases, viral infections and various cancers. The nucleic acid needs to be delivered across the cell membrane and into the nucleus to affect the gene expression. Anionic nucleic acids need a cationic carrier, such as a cationic liposome, to enable their delivery into the cells. The liposomes used in gene delivery usually contain both a cationic lipid to associate with the nucleic acid and a neutral helper lipid to stabilize the structure. The liposome-nucleic acid complex is called a lipoplex. The cationic carrier must include or function as a cell-penetrating enhancer (CPE) to be able to translocate across the cell membrane into the cytosol and to the nucleus.

The experimental part of this work was aimed at developing and characterizing an innovative poly-cationic liposomal platform for gene delivery, using a novel synthetic CPE. The CPE used in this study is an oligo-guanidyl derivative (OGD) that had either 4 (OGD4) or 6 (OGD6) cationic charges. Liposomes were surface-engineered with OGD, obtaining a cationic formulation that was then exploited for DNA loading. The study has two main characterization steps: Step 1 was to decorate liposomes with OGD by post insertion using increasing amounts of OGD, and determine the vesicle size and zeta potential by dynamic light scattering (DLS). Step 2 involved DNA loading by post insertion into the cationic liposomes with increasing amounts of DNA. The lipoplex size and zeta potential was determined by DLS, the complexation by electrophoresis, and the thermodynamics of the cationic liposome/DNA association by isothermal titration calorimetry (ITC). The measurements were performed in isotonic buffers (HEPES pH 7.4 and citrate pH 5) and in lower ionic strength TRIS buffer (pH 7.4).

The aim of the characterization studies was first to find a liposome composition that includes just enough OGD to obtain a sufficiently high zeta potential and a uniform, sufficiently small size. The optimal formulation contained either 10 % of OGD4 or 5 % of OGD6 of the total lipid amount. The second step was to find the highest stable DNA loading for the lipoplexes. All the characterization studies were performed on OGD4 lipoplexes in TRIS buffer. The optimal OGD4/DNA N/P (nitrogenous/phosphorous) ratio was found to be around 5.

Further investigation is needed to determine the best lipoplex composition and manufacturing method using an isotonic buffer. A DNA release study remains to be performed prior to further *in vitro* and *in vivo* studies.

Avainsanat – Nyckelord – Keywords

Lipoplex, gene delivery, dynamic light scattering (DLS), electrophoresis, isothermal titration calorimetry (ITC)

Säilytyspaikka – Förvaringställe – Where deposited

Division of Pharmaceutical Biosciences

Muita tietoja – Övriga uppgifter – Additional information

Supervisors: Stefano Salmaso and Tapani Viitala

HELSINGIN YLIOPISTO
HELSINGFORS UNIVERSITET
UNIVERSITY OF HELSINKI

Tiedekunta/Fakultet – Faculty	Osasto/Sektion– Department	
Farmasian tiedekunta	Farmaseuttisten biotieteiden osasto	
Tekijä/Författare – Author		
Maria Laakko		
Työn nimi/Arbetets titel – Title		
Uudet kationiset lipopleksit geenien annostelussa		
Oppiaine /Läroämne – Subject		
Biofarmasia		
Työn laji/Arbetets art – Level	Aika/Datum – Month and year	Sivumäärä/ Sidoantal – Number of pages
Pro gradu	Toukokuu 2017	60 + 1

Tiivistelmä/Referat – Abstract

Geeniterapia on nukleiinihappojen annostelua kohdesoluihin, joissa ne korvaavat puuttuvan, vaurioituneen tai heikosti ilmentyvän geenin. Geeniterapia voisi tulevaisuudessa toimia vaikeiden sairauksien, kuten geneettisten sairauksien, virusinfektioiden tai useiden syöpien, hoitomuotona. Nukleiinihapon tulee läpäistä solukalvo ja päästä tumaan vaikuttaakseen geenien ilmentymiseen. Negatiivisesti varautuneet nukleiinihapot tarvitsevat positiivisesti varautuneen kantajan, kuten kationisen liposomin, päästäkseen solujen sisään. Geenien annostelussa käytetyt liposomit sisältävät yleensä kationisen lipidin, johon nukleiinihappo kiinnittyy, ja neutraalin apulipidin stabiloimaan rakennetta. Liposomi-nukleiinihappokompleksia kutsutaan lipopleksiksi. Kationisen kantajan tulisi sisältää tai toimia lisäksi soluun pääsyn edistäjänä (cell-penetrating enhancer, CPE), joka auttaa nukleiinihappoa siirtymään solukalvon läpi ja edelleen tumaan.

Työn kokeellisessa osuudessa kehitettiin ja tutkittiin uutta polykationista liposomialustaa geenien annosteluun, käyttäen uutta synteettistä CPE:tä. Tässä tutkimuksessa käytetty CPE on oligo-guanidyylijohdannainen (OGD), jolla on joko 4 (OGD4) tai 6 (OGD6) kationista varausta. Liittämällä liposomiin OGD:tä saatiin positiivisesti varautunut formulaatio, joka sitten lastattiin DNA:lla. Karakterisointi sisälsi kaksi vaihetta. 1. vaihe oli OGD:n liittäminen valmiisiin liposomirakkuloihin kasvavina määrinä ja rakkulan koon sekä zetapotentiaalin määritys dynaamisella valosirontamenetelmällä (DLS:llä). 2. vaihe sisälsi DNA:n lastaamisen kationiseen liposomiin kasvavina määrinä. Lipopleksin koko ja zetapotentiaali määritettiin DLS:llä, kompleksoituminen elektroforeesilla ja sitoutumisen termodynamiikka isotermaalisella titraatiokalorimetrialla (ITC:llä). Mittauksia tehtiin sekä isotonisilla puskureilla (HEPES pH 7.4 ja sitraatti pH 5) että pienemmän ionivahvuuden TRIS-puskurilla (pH 7.4).

Karakterisoinnin tavoitteena oli löytää liposomiformulaatio, jossa pienimmällä mahdollisella määrällä OGD:tä saatiin riittävän korkea zetapotentiaali sekä riittävän pieni ja tasainen partikkelikoko. Optimaalinen formulaatio sisälsi joko 10 % OGD4:ä tai 5 % OGD6:a kokonaisliposomien määrästä. Toisena tavoitteena oli selvittää, kuinka suuri määrä DNA:ta kompleksoituu kationiseen liposomiin. OGD4-lipoplekseille TRIS-puskurissa tehtiin kaikki analyysit. OGD4:n ja DNA:n optimaaliseksi N/P (typpi/fosfori) suhteeksi saatiin noin 5.

Lisätutkimuksia tarvitaan selvittämään paras lipopleksien valmistusmenetelmä ja koostumus isotonisessa puskuriliuoksessa. Lisäksi DNA:n vapautumiskokeet pitää tehdä ennen *in vitro*- ja *in vivo*-lisätutkimuksia.

Avainsanat – Nyckelord – Keywords

Lipopleksi, geenien annostelu, dynaaminen valosironta (DLS), elektroforeesi, isotermaalinen titraatiokalorimetria (ITC)

Säilytyspaikka – Förvaringställe – Where deposited

Farmaseuttisten biotieteiden osasto

Muita tietoja – Övriga uppgifter – Additional information

Ohjaajat: Stefano Salmaso ja Tapani Viitala

ACKNOWLEDGEMENTS

The experimental part of my Master's thesis was done in the Department of Pharmaceutical and Pharmacological Sciences in the University of Padova in Italy. This research project was an integral part of the research collaboration between Dr. Tapani Viitala's and Prof. Stefano Salmaso's research groups.

First, I want to thank my supervisors Dr. Tapani Viitala and Prof. Stefano Salmaso for enabling this work. I am very grateful for Dr. Viitala's and Prof. Marjo Yliperttula's support and guidance during the project. Special thanks to Alessio Malfanti for tutoring and helping me in the laboratory.

I am grateful for Elena Ambrosio's help in performing the ITC measurements. Thank you, Silvia Gallina, for peer support. Also, thanks to Dr. Anna Balasso for your help in analyzing the liposomes. I am sincerely grateful to the whole research group in Prof. Salmaso's laboratory, you made my stay and work fun, and also helped me learn Italian.

Special thanks to my family Leena, Ilkka and Eveliina for endless support over the years. I want also to thank my friends who have been there for me when I have needed them. My greatest gratitude is dedicated to my friend Ville who reviewed the text, supported and encouraged me, and gave me constructive criticism during the work.

Helsinki, May 2017

Maria Laakko

TABLE OF CONTENTS

1 INTRODUCTION 1
2 LITERATURE REVIEW 2
2.1 Lipoplexes 2
2.1.1 Liposomes 2
2.1.2 Cationic liposomes in gene delivery 6
2.1.3 Lipofectamine 8
2.2 Cell-penetrating enhancers 8
2.2.1 Cell penetrating peptides 8
2.2.2 Applications of cell-penetrating peptides in gene delivery 9
2.2.3 Novel non-peptide cell-penetrating enhancer 10
2.3 Characterization methods 11
2.3.1 Dynamic Light Scattering for particle size measurements 11
2.3.2 Zeta potential 15
2.3.2 One-dimensional gel electrophoresis 18
2.3.3 Isothermal titration calorimetry 20
3 AIM OF THE STUDY 22
4 MATERIALS AND METHODS 23
4.1 Novel cationic lipoplexes 23
4.2 Buffer preparation 25
4.3 Liposome preparation and different characterization methods 28
4.3.1 Post-insertion of oligo-guanidyl derivative 29
4.3.2 Post-insertion of double stranded DNA 30
4.3.2 Size and zeta potential measurements with dynamic light scattering 30
4.3.3 Electrophoretic mobility shift assay 31
4.3.4 Isothermal titration calorimetry 33
5 RESULTS 34
5.1 Dynamic light scattering results for OGD4 34
5.2 Electrophoretic mobility shift assay for OGD4 41
5.3 Isothermal titration calorimetry for OGD4 41
5.4 Dynamic light scattering results for OGD6 46
5.5 Electrophoretic mobility shift assay for OGD6 50
6 DISCUSSION 50
6.1 Characterization studies 50
6.2 Future perspectives 53
7 CONCLUSION 54
BIBLIOGRAPHY 56

APPENDIX A: Isothermal titration calorimetry raw data

LIST OF ABBREVIATIONS

APS	ammonium persulfate
CPE	cell-penetrating enhancer
CPP	cell-penetrating peptide
DLS	dynamic light scattering
DNA	deoxyribonucleic acid
dsDNA	double stranded DNA
DOPE	Dioleoylphosphatidylethanolamine
EDL	electric double layer
EDTA	ethylenediaminetetraacetic acid
EggPC	egg phosphatidylcholine
FBS	fetal bovine serum
HEPES	4-(2-hydroxyethyl)-1-piperazineethanesulfonic acid
HSPC	hydrogenated soy phosphatidylcholine
ITC	isothermal titration calorimetry
LUV	large unilamellar vesicles
MPS	mononuclear phagocyte system
OGD	oligo-guanidyl derivative
PEG	polyethylene glycol
RES	reticuloendothelial system
RNA	ribonucleic acid
siRNA	small interfering RNA
sla-DLS	single large scattering angle DLS
SUV	small unilamellar vesicles
TAT	trans-activator of transcription
TBE	TRIS, boric acid and EDTA
TEMED	N,N,N′,N′-tetramethylethylenediamine
TRIS	2-Amino-2-(hydroxymethyl)-1,3-propanediol base

1 INTRODUCTION

Gene therapy is the therapeutic delivery of nucleic acid sequences into cells (Alhakamy et al. 2013). It is a potential treatment to cure e.g. genetic diseases, viral infections and various cancers. Research in this field has become popular and it has seen remarkable development in recent years (Nayerossadat et al. 2012; Alhakamy et al. 2013). The genetic material needs to be delivered across the cell membrane and into the nucleus using either a viral or a non-viral vector as a delivery system. This Master's thesis focus on the non-viral vectors, especially liposomes.

In general, anionic oligonucleotides, such as deoxyribonucleic acid (DNA) and ribonucleic acid (RNA), need a cationic carrier to enable their delivery into the cells (Nayerossadat et al. 2012; Alhakamy et al. 2013). The cationic carrier must include a cell-penetrating enhancer (CPE) to be able to translocate across the cell membrane into the cytosol and to the nucleus. The liposomes used in gene delivery usually contain both a cationic lipid to associate with the DNA or RNA and a neutral helper lipid to stabilize the structure. The liposome-oligonucleotide complex is called a lipoplex. The cell penetrating enhancer can be either peptide-based (a cell penetrating peptide (CPP)) or a non-peptide molecule with cell penetrating properties (Bersani et al. 2012).

In this thesis, a novel cationic synthetic cell penetrating enhancer designed to anchor to either liposomal or polymer carriers is used (Bersani et al. 2012). The novel CPE is first anchored to a liposomal platform and then DNA is introduced to the surface-engineered liposomes to create a lipoplex. Studies concerning the manufacturing of the cationic liposomes, their physico-chemical properties, and their association to DNA by using various techniques are performed.

The literature review of this Master's thesis focuses on the materials and characterization methods used in this study. Liposome structure, cell penetrating enhancers, and the use of cationic liposomes in gene delivery are explained. This is followed by an overview of the measurement techniques used: dynamic light scattering, zeta potential, mobility shift electrophoresis and isothermal titration calorimetry. The experimental part is focused on

characterizing the novel cationic liposome composition and their DNA association properties using the aforementioned techniques. This Master´s thesis is then concluded with the summary of the results and suggestions for further studies.

2 LITERATURE REVIEW

This literature review gives a general overview of the materials and the measurement techniques relevant to this study, specifically liposomes, lipoplexes, cell penetrating peptides, dynamic light scattering, zeta potential, gel electrophoresis and isothermal titration calorimetry.

2.1 Lipoplexes

2.1.1 Liposomes

Liposomes are spherical lipid vesicles whose dimension varies from 30 to 2500 nm, and are classified according to their diameter and structure (Akbarzadeh et al. 2013; Allen and Cullis 2013). Liposomes are classified in multilamellar and unilamellar vesicles as shown in Figure 1. There are also two categories of unilamellar vesicles: large unilamellar vesicles (LUV) and small unilamellar vesicles (SUV). Unilamellar vesicles have a single lipid bilayer, while multilamellar vesicles can have several lipid bilayers. The basic structure of a unilamellar vesicle is shown in Figure 2. LUVs are prepared by extrusion through polycarbonate filters from multilamellar vesicles. Multilamellar vesicles need to be sonicated before the extrusion to obtain SUVs. Liposomes can also be classified by composition and mechanism of drug delivery to conventional, long-circulating, polymorphic (pH-sensitive, thermosensitive, and cationic liposomes), and decorated liposomes (surface-modified liposomes and immunoliposomes) (Lopes et al. 2013).

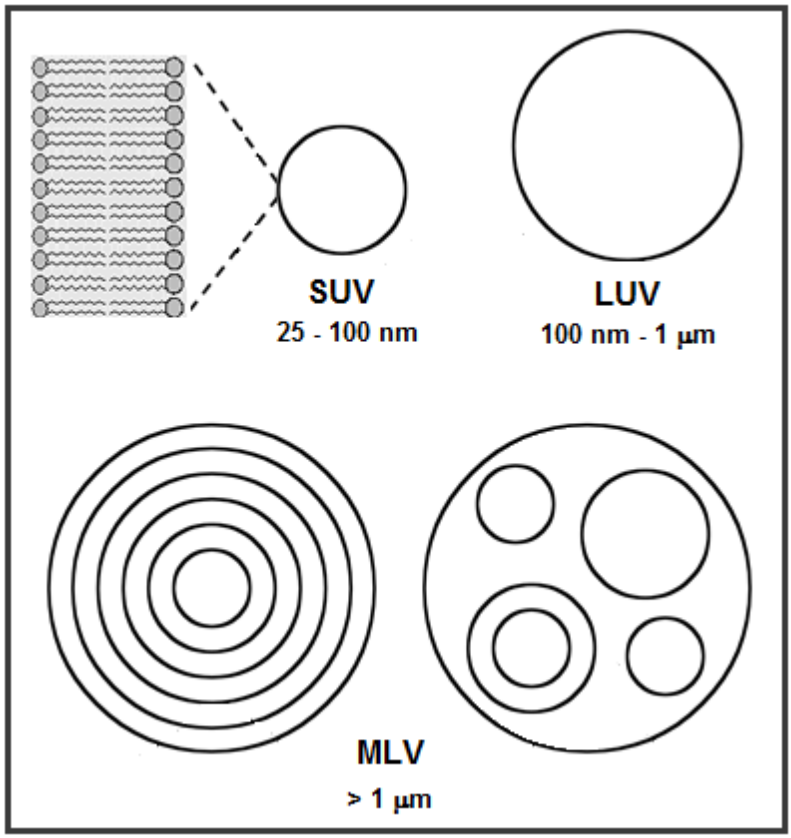

Figure 1. Liposome classification: Multilamellar vesicles on the bottom and two types of unilamellar vesicles and their vesicle diameter on the top of the figure (Lopes et al. 2013).

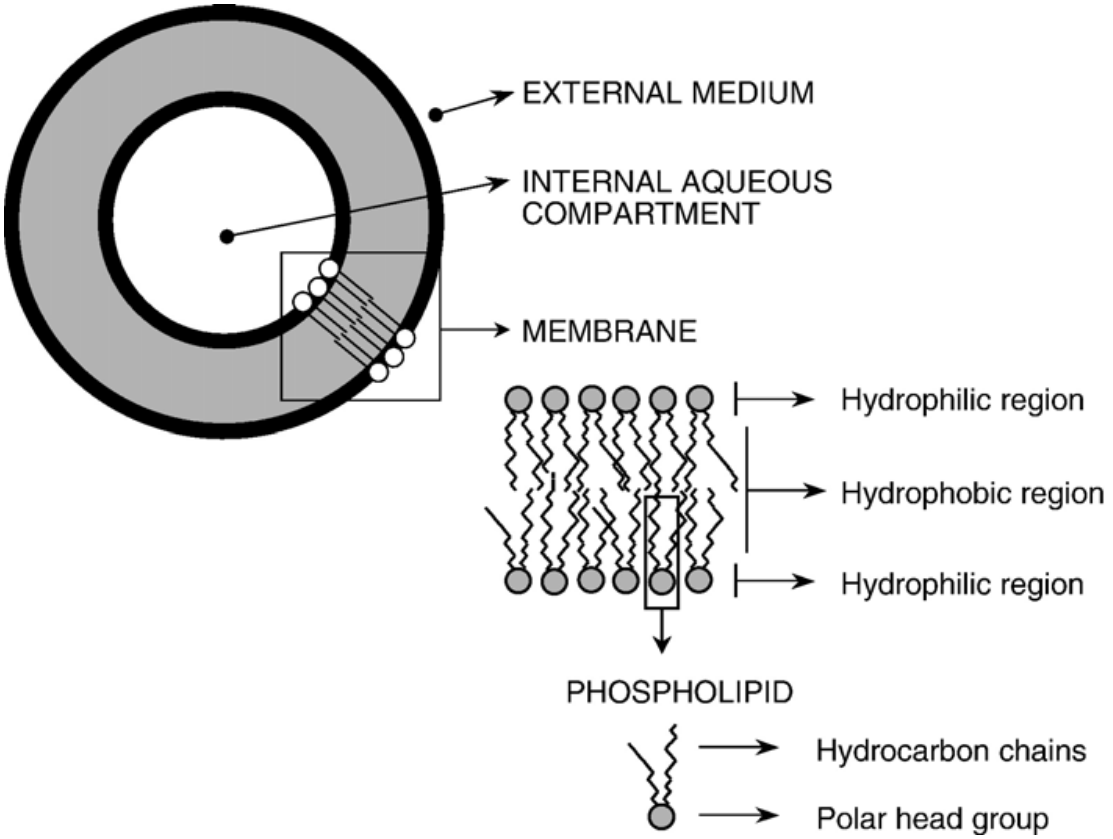

Figure 2. The basic structure and composition of unilamellar liposomes (Frézard et al. 2007).

Bangham et al. (1965) were the first to discover liposomes in the 1960s when they studied swollen phospholipid systems that became the basic model of membrane systems. In their study, they discovered that the phospholipids form hollow vesicles with a phospholipid bilayer where the polar heads are oriented towards the interior and exterior aqueous phases and the lipophilic tails heading inside the lipid bilayer. At the beginning of 1970s Gregoriadis (1973) discovered that both water-soluble and lipid-soluble substances can be entrapped in the aqueous or lipid phase of liposomes, respectively. The elimination time from the blood for liposome-entrapped drugs is longer than for non-entrapped drugs. They studied liposomes that contained a phospholipid, cholesterol and either stearylamine (cationic liposomes) or phosphatidic acid (anionic liposomes).

Liposomes have many advantages, such as biocompatibility, biodegradability, low toxicity, and ability to trap both hydrophilic and lipophilic compounds (Akbarzadeh et al. 2013). Therefore, liposomes are becoming more common as a drug delivery system. Liposomes can also reduce drug toxicity, increase efficacy and therapeutic index of drugs,

increase stability, reduce the exposure of sensitive tissues to toxic drugs, and help targeting specific cells. Of course, liposomes have also some disadvantages that need to be considered when using it as a drug carrier. These are low solubility, short half-life, leakage and fusion of encapsulated drugs or molecules, high production cost, and sometimes the phospholipids experience oxidation and hydrolysis-like reactions.

The drugs can be loaded to liposomes either passively during the liposome formation or actively after the liposome formation (Akbarzadeh et al. 2013; Allen and Cullis 2013). Lipid-soluble drugs can be passively combined into liposomes during vesicle formation. Instead, passive loading during vesicle formation of water-soluble drugs is depending on the ability of liposomes to entrap aqueous buffer that contains the drug. Loading after the liposome formation is active and independent of the time and site of liposome manufacture. Water-soluble drugs can be loaded actively to liposome by the effect of pH gradient. The drug retention in liposomes is drug dependent.

Conventional liposomes are not very stable *in vivo* because of their rapid clearance from circulation by the mononuclear phagocytic system (MPS), also known as reticuloendothelial system (RES) (Allen and Cullis 2013). Circulation half-life can be extended by using large doses of empty liposomes before introducing liposomes with the drug, or by reducing the vesicle size. The first long circulating liposomes, that did not need MPS blockade to achieve the effect, were composed of egg phosphatidylcholine (EggPC) and cholesterol, and addition of the monosialylganglioside GM1. A simpler way to prepare long circulating liposomes is to coat them with polyethylene glycol (PEG) (Akbarzadeh et al. 2013; Allen and Cullis 2013). PEG coating helps avoiding liposome recognition by the MPS because it inhibits protein adsorption and opsonization of liposomes (Gabizon 2001). These long circulating liposomes are called stealth liposomes. They have a phospholipid bilayer as a membrane and are used for drug or gene delivery into cells (Akbarzadeh et al. 2013; Allen and Cullis 2013). It has been discovered that PEG-liposomes have dose-independent clearance at normal doses.

Intracellular delivery of drugs is both a limitation and a benefit for liposomal drug carriers (Akbarzadeh et al. 2013; Allen and Cullis 2013). For macromolecules, such as small

interfering RNA (siRNA), and peptides that do not enter cells on their own, intracellular delivery is an essential prerequisite to achieve therapeutic activity. There is two ways to mediate this internalization, either by including antibodies or other ligands or via fusogenic agents. Liposomes interact with cells mainly by adsorption or endocytosis. A less common type of liposomal interaction with cells is fusion with the cell membrane. These liposomes contain fusogenic lipids or membrane-active peptides that can disrupt the cell membrane to induce the cytoplasmic delivery of the drug. When the therapeutic molecule can survive the acidic and enzyme-rich environment of the endosomes and lysosomes, then the most common way to introduce molecules into the cell interior is receptor-mediated endocytosis of ligand-targeted liposomes. Antibodies are usually used as a ligand for targeted liposomes. These antibody-targeted liposomes can improve the selective toxicity of anticancer agents but, their *in vivo* distribution to non-MPS tissues is limited by rapid clearance form circulation. Ligand-targeted liposomes do not have many advantages over passively targeted (i.e. 'non'-targeted) liposomes, and improvements in survival are often due to increased receptor-mediated uptake of the liposomes containing the entrapped drug.

2.1.2 Cationic liposomes in gene delivery

Gene therapy is the therapeutic delivery of large nucleic acid macromolecules (Alhakamy et al. 2013). It has become a popular research topic because of its potential to treat severe and challenging diseases, such as genetic diseases, viral infections and various cancers. In gene therapy, genetic material can be delivered into a target cell to replace a gene that is missing, mutated or poorly expressed. Alternatively, siRNA can be used to silence the expression of specific genes.

When cationic liposomes or micelles are complexed with oligonucleotides, such as double stranded DNA (dsDNA) and siRNA, the complex is called a lipoplex (Nayerossadat et al. 2012). Lipoplexes and polyplexes (the complex between a cationic polymer and nucleic acids) can act as chemical non-viral delivery systems for genes. Non-viral delivery systems are less efficient than viral systems in gene transduction, but their advantages compared to viral systems are cost-effectiveness, availability, lower induction

of the immune system, and no limitation on the size of the transgenic DNA. Besides, cationic liposomes are less toxic and antigenic than viral vectors or other non-viral delivery systems because they are made of only biological lipids. The positive charge on the cationic liposome surface develops an electrostatic interaction with the negatively charged nucleic acids and facilitates contact with the negatively charged cell membranes (Dalby et al. 2004). Cationic polymers vary from cationic lipids, since they do not contain a hydrophobic moiety and are completely soluble in water (Tros de Ilarduya et al. 2010). They can also be synthesized in different lengths and geometries. It is also possible to add functional groups to polymers with relative ease and flexibility.

Cationic liposomes are at present the most essential non-viral polycationic systems for gene delivery (Nayerossadat et al. 2012). Cationic liposomes are usually composed of a cationic lipid, i.e. DOTAP (1,2-dioleoyl-3-trimethylammonium-propane (chloride salt)), and a neutral lipid, i.e. dioleoylphosphatidylethanolamine (DOPE) or cholesterol. Their unique characteristics include the capability to incorporate both hydrophilic and hydrophobic drugs, low toxicity, no immune system activation, and targeted delivery of bioactive compounds to the site of action. As mentioned earlier, the disadvantages of liposomes are their rapid elimination by RES and their inability to achieve constant drug delivery over a prolonged period of time. These issues can be overcome by coating the liposomes with PEG or integrating the pre-encapsulated drug-loaded liposomes within depot polymer-based systems.

Cholesterol or DOPE is usually used as a helper lipid when using liposomes for gene delivery to facilitate the lipid exchange and membrane fusion between lipoplexes and the endosomal membrane by unstabilizing it (Nayerossadat et al. 2012). Cationic liposomes that contained cholesterol as a helper lipid are structurally more stable in physiologic media (Tros de Ilarduya et al. 2010). Therefore, cholesterol containing lipoplexes can reach their target tissue flawlessly, protect the DNA from degradation, and facilitate transfection. The efficiency of gene delivery in liposomes depends on the size, structure, and charge ratio between the oligonucleotide and the cationic liposome, presence of a helper lipid, and the cell type.

2.1.3 Lipofectamine

Lipofectamine is a commercial cationic liposome based reagent that has a high transfection efficiency for nucleic acids (Dalby et al. 2004; Cardarelli et al. 2016). Lipofectamine can complex and carry negatively charged nucleic acid molecules. It also allows them to overcome the electrostatic repulsion of the cell membrane and to be taken up by the cell. In RNA interference studies, synthetic siRNA has been transfected into mammalian cells by using Lipofectamine 2000.

In a recent study Rasoulianboroujeni et al. (2017) demonstrated that cationic liposomes can be used to transfect and express the LacZ-gene (part of the E. coli *lac* operon) approximately equally to Lipofectamine 2000. Their cationic liposomes consisted of DOTAP/DOPE/cholesterol with a molar ratio of 1:1:2, and they used a modified lipid film hydration method consisting of a lyophilization step for gene delivery applications.

2.2 Cell-penetrating enhancers

2.2.1 Cell penetrating peptides

Cell-penetrating peptides (CPPs) are short arginine-rich amino acid sequences (less than 30 amino acids) that can translocate the cellular membranes and access the cell interior (Järver and Langel 2006; Herce and Garcia 2007; Herce et al. 2014). CPPs can descend from naturally occurring peptide sequences or be synthetized *ex novo*. They are also known as protein transduction domains (PTDs), Trojan peptides or membrane translocating sequences (MTS). CPPs can carry a wide range of different sized bioactive molecules such as proteins, peptides, oligonucleotides, and even 200 nm nanoparticles like liposomes (Torchilin et al. 2001; Järver and Langel 2006; Herce and Garcia 2007). They have a large net positive charge and therefore they can penetrate almost any cell. Significant differences between different CPPs are size, amino acid sequence, and charge, but their common characteristics are the ability to rapidly translocate the plasma membrane and enable the delivery of their payload to the cytoplasm or nucleus (Järver and Langel 2006).

The first observation of CPPs was made in 1988, when the trans-activator of transcription (TAT) protein was isolated from the HIV-1 virus (Frankel and Pabo 1988). The TAT protein was shown to have the ability to enter the cells and translocate to the nucleus. The cellular uptake can follow two different pathways: translocation across the cell membrane directly (energy-independent pathway) or endocytosis followed by release into the cytosol (energy-dependent pathway) (Järver and Langel 2006; Herce and Garcia 2007). Early studies on CPP translocation suggested that they use an energy-independent pathway to translocate across the cell membrane. These suggestions were based on low temperature (4 °C) studies, which inhibit the cellular adenosine triphosphate (ATP) pool, or on chemically inhibiting the endocytosis receptors. However, later studies have shown that some mechanisms of CPP translocation involve extracellular heparan sulfate and endocytosis and are therefore mostly energy-dependent. The translocation pathway of CPPs depends on their cargo and biophysical properties, even though it seems that the endosomal pathway is the major route of uptake.

2.2.2 Applications of cell-penetrating peptides in gene delivery

CPPs can be used to enhance the cellular uptake of different biomolecules or vectors such as oligonucleotides, liposomes, peptides, proteins and viruses (Alhakamy et al. 2013). Non-viral vectors have difficulties in overcoming the barriers between the administration site and the nuclei of the target cells. These barriers include, for example, efficient cellular uptake, chemical stability of the genetic material and its delivery vesicle, and escape from the endosomal network before degradation within lysosomes. To achieve efficacious non-viral gene delivery the challenge is to overcome these barriers. CPPs can transport various biomolecules across the cell membrane, and therefore they are an attractive option for helping non-viral vectors in gene delivery to overcome some of the barriers.

Positively charged CPPs interact through electrostatic interaction with the negatively charged oligonucleotides (e.g. dsDNA and siRNA) (Alhakamy et al. 2013). This process helps to condensate the genetic material and protect it from nuclease enzyme digestion.

It can also lead to small nanoparticles with a net positive charge that is able to interact with negatively charged moieties on cell surfaces.

Cellular uptake of CPP nanoparticles is influenced by the chemical nature of cationic residues (Alhakamy et al. 2013). Arginine-rich CPPs tend to be more efficient than lysine-rich CPPs in mediating the cell uptake. Polyarginine peptides can interact electrostatically with both siRNA and dsDNA. For delivery of genetic material and condensation of oligonucleotides into stable complexes it would be good to have a chain of at least six amino acids. Usually four-five arginine residues are involved in forming the complexes with oligonucleotides, and the extra arginine residues are available for interaction with the cell membrane. Transfection efficiency can be increased to reach the same order of magnitude as that of Lipofectamine 2000 by introducing a hydrophobic group to the CPPs.

2.2.3 Novel non-peptide cell-penetrating enhancer

The use of CPPs in drug delivery has some difficulties such as unspecific cell delivery, low stability, and intrinsic biological activity (Bersani et al. 2012). Bersani et al. (2012) decided to try to overcome these problems by designing a novel non-peptide CPE, hepta-arginyl-*N*-acetyl-maltotriosylamido-dodecanoic acid (Arg_7-Malt-$NAcC_{12}$ acid). It is a non-linear oligo-arginyl with an unusual star-like structure, designed for conjugation to large systems, e.g. proteins, oligonucleotides or colloidal drug carriers, to promote their cell entry. The star-like CPE contains a variable number of arginine functions attached to a maltotriose anchoring structure. By simple chemical protocols the hydroxyl groups of the maltotriose can provide for multiple derivatizations with arginyl residues. The guanidinium headgroup of arginine is essential for cellular uptake because it interacts with membrane phospholipids. Therefore, the novel enhancers were designed to resemble the oligo-arginine structure of the TAT transduction domain. The cell translocation of the guanidium-rich structures is three times faster than that of TAT. This is because the insertion of the novel enhancers into lipid bilayers produces a local membrane distortion leading to transient pore formation on the membrane. Arg_7-Malt-$NAcC_{12}$ acid can be covalently or electrostatically combined with colloidal therapeutic systems to promote

their cellular uptake. The cell penetrating properties of Arg_7-Malt-$NAcC_{12}$ acid derivative were evaluated to compare it to other CPPs by labeling the molecules with fluorophores, such as fluorescein or rhodamine. Quantitative fluorescence studies and cytofluorimetric analyses showed that Arg_7-Malt-$NAcC_{12}$ acid can enter both the human MCF-7 breast adenocarcinoma and murine MC3T3-E1 embryonic fibroblast cell lines.

2.3 Characterization methods

2.3.1 Dynamic Light Scattering for particle size measurements

One of the most commonly mentioned factors that are responsible for a range of biological effects of nanoparticles is particle size (Bhattacharjee 2016). Dynamic Light Scattering (DLS), also known as Photon Correlation Spectroscopy or Quasi-Elastic Light Scattering, is a popular tool within the pharmacy community. DLS is non-invasive, requires minimal sample preparation and no pre-experimental calibration. The instruments are integrated, compact, affordable and user-friendly. A selection of light scattering instruments such as Malvern Zetasizer series, Brookhaven NanoDLS series, and Microtrac Wave II series have appeared in recent years. In this study, the single large scattering angle DLS (sla-DLS) Malvern Zetasizer nanoZS 173° was used. The sla-DLS technique is explained below.

DLS measures Brownian motion, which is the random movement of particles in a liquid (Technical note 2016). The larger the particles are the slower the Brownian motion. The motion of the particles causes the observed intensity of the scattered light to fluctuate. The typical scattered intensity fluctuation for large and small particles is illustrated in Figure 3. DLS measures the autocorrelation function of the scattered intensity and then fits it with a mathematical model to determine the translational diffusion coefficient D of the scattering particles, as well as their polydispersity index (PDI). D is related to the hydrodynamic diameter d(H) of the particles via the Stokes-Einstein equation,

$$d(H) = \frac{kT}{3\pi\eta D}, \quad (1)$$

where k is the Boltzmann's constant, T is the absolute temperature of the sample, and η is the viscosity of the solvent.

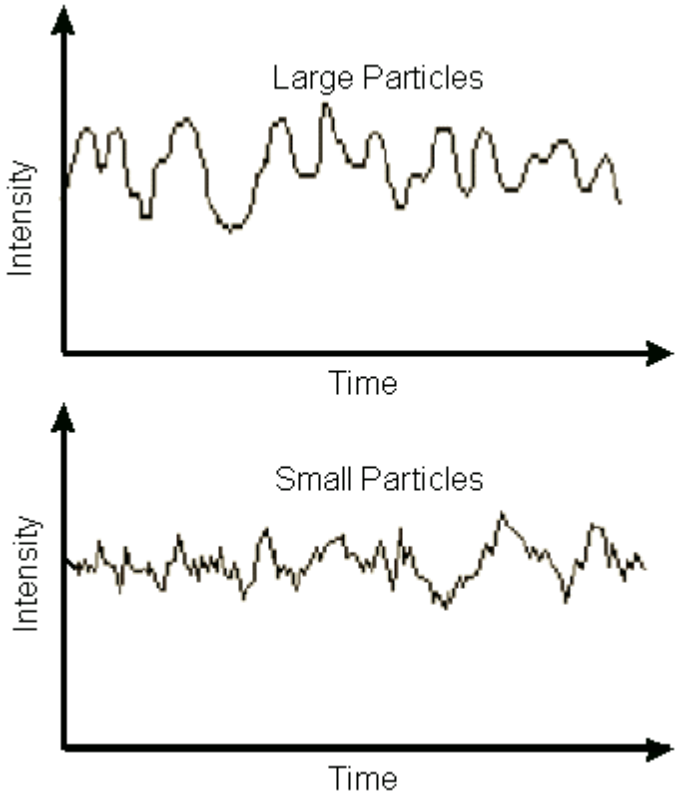

Figure 3. A typical intensity fluctuation for large and small particles in DLS (Technical note 2016).

The measured hydrodynamic diameter is affected by the size of the particle core, the surface structure, the concentration and the ionic strength of the medium (Technical note 2016). The thickness of the electric double layer called the Debye length (κ^{-1}) can change in different ionic concentration which then affect the particle diffusion speed. The changes in the particle surface that affect the diffusion speed change also the apparent size of the particle. The changes in the shape of a particle can affect the diffusion speed and thus the computed hydrodynamic size. For example, if the diameter of a rod shaped particle changes it does not noticeably affect the diffusion speed but changes in the particle length will.

The sla-DLS instruments have three major components, a laser, the sample and a light detector, which are shown in Figure 4 (Bhattacharjee 2016). The Malvern Zetasizer Nano system uses a laser with a wavelength of 633 nm and either a 173° or 90° detector angle (Technical note 2016). Correspondingly the NanoDLS series uses a laser with a

wavelength of 638 nm and a 90° detector angle (Brookhaven Instruments 2016). The 173° detector angle is also known as backscatter detection and it excludes excess scattered light (Bhattacharjee 2016; Technical note 2016). In DLS the autocorrelation function is fitted with two different mathematical algorithms, either using the cumulant method or the CONTIN algorithm (Bhattacharjee 2016). The cumulant method is unsuitable for heterogeneous polydisperse (particles of varied size in a disperse system) samples and therefore the CONTIN algorithm is preferred (Varga et al. 2014; Bhattacharjee 2016). Since samples are rarely monodisperse (particles of uniform size in a disperse system), the results obtained using the two algorithms differ (Bhattacharjee 2016). The PDI estimates the width of the particle size distribution. When the PDI ≤ 0.1 the sample is considered to be highly monodisperse, and when it is 0.1–0.4 and > 0.4 the sample is considered to be moderately and highly polydisperse, respectively. If the PDI is higher than 0.7 the DLS technique might not give reliable size results.

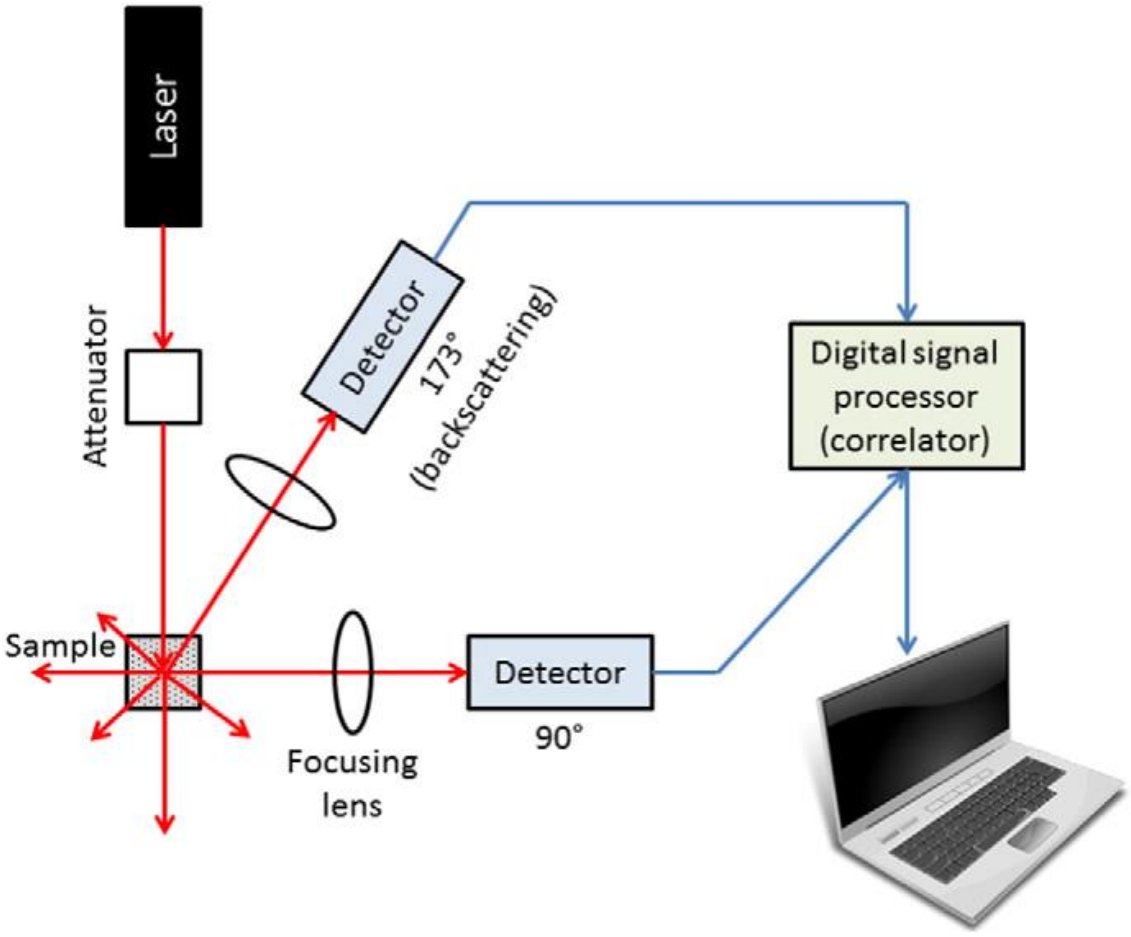

Figure 4. Schematic diagram of the instrumentations of dynamic light scattering (DLS) (Bhattacharjee 2016).

The size of the nanomedicine is one of the factors that influences its biodistribution after entry in the body and therefore the size measurement is crucial for the characterization of the nanomaterial (Gaumet et al. 2008). Varenne et al. (2015) standardized and validated a protocol of size measurements by DLS for monodisperse stable nanomaterial characterization. In the validation of the protocol they studied robustness, repeatability, intermediate precision, trueness, and measurement uncertainty for 60 nm and 200 nm nanoparticles at 20 °C and 25 °C. The 200 nm particles (close to the size of the particles used in this study) were liposomes that contained either egg phosphatidylcholine (EggPC) or cholesterol and EggPC. The robustness study included the influence of the temperature of the sample, the influence of the analyst, and the volume of the sample. The results showed that the temperature of the sample should be within −5 °C of 25 °C and within ±2.5 °C of 20 °C when the equilibration time is 300 seconds. The influence of the analyst and the volume of the sample was evaluated on each standard by using different analysts and the minimum and maximum volumes of the cuvette recommended by the supplier of the instrument at each temperature. Different analysts or volumes did not cause a statistical difference between the size measurements. A procedure is considered to meet the requirements when the relative standard uncertainly for the mean value from each size measurement is less than 5% according to the ISO 22412:2008 standard (International Organization for Standardization 2008). The validation protocol was also shown to have good repeatability (Varenne et al. 2015). The trueness was studied using two latex particle materials with SI-traceable certified values of 60 and 203 nm obtained by transmission electron microscopy. They are spherical nanoparticles that do not swell in aqueous dispersions, and appear quite monodisperse by the low PDI (PDI<0.05). The threshold of trueness was set at 10% since it was not indicated in the ISO standard. The relative standard uncertainty of trueness was less than this threshold for all the cases they studied. The confidence interval determined by combining all sources of measurement uncertainty was found to meet the standards that were set to this study.

Several studies have used DLS to determine the hydrodynamic size of liposomes (Stiufiuc et al. 2015; Kerek and Prenner 2016; Sebaaly et al. 2016; Zuo et al. 2016). Most of them have used sla-DLS instruments that use either 90° or 173° scattering angles (Stiufiuc et al. 2015; Kerek and Prenner 2016; Sebaaly et al. 2016). The sla-DLS instruments are

typically used because the influence of potential “dust contaminations” on the correlation functions is significantly reduced (Fischer and Schmidt 2016). Fischer and Schmidt (2016) discovered in their study that the size determination by sla-DLS almost always yields too small radii when measuring particles such as lipoplexes that exhibit a wide size distribution.

2.3.2 Zeta potential

Surface charge is another factor that is responsible for a range of biological effects of nanoparticles (Bhattacharjee 2016). Zeta potential, also known as the electrokinetic potential, is the potential at the shear or slipping plane of a charged colloidal particle that moves towards the oppositely charged electrode owing to electrophoresis (Kaszuba et al. 2010). The electric double layer (EDL), shown in Figure 5, is formed when a diffuse layer consisting of both same and opposite charged ions/molecules grows beyond the Stern layer due to the electrostatic field of the charged nanoparticles (Kaszuba et al. 2010; Bhattacharjee 2016). The diffuse layer composition is dynamic and varies depending on a variety of factors such as pH, ionic strength, concentration etc.

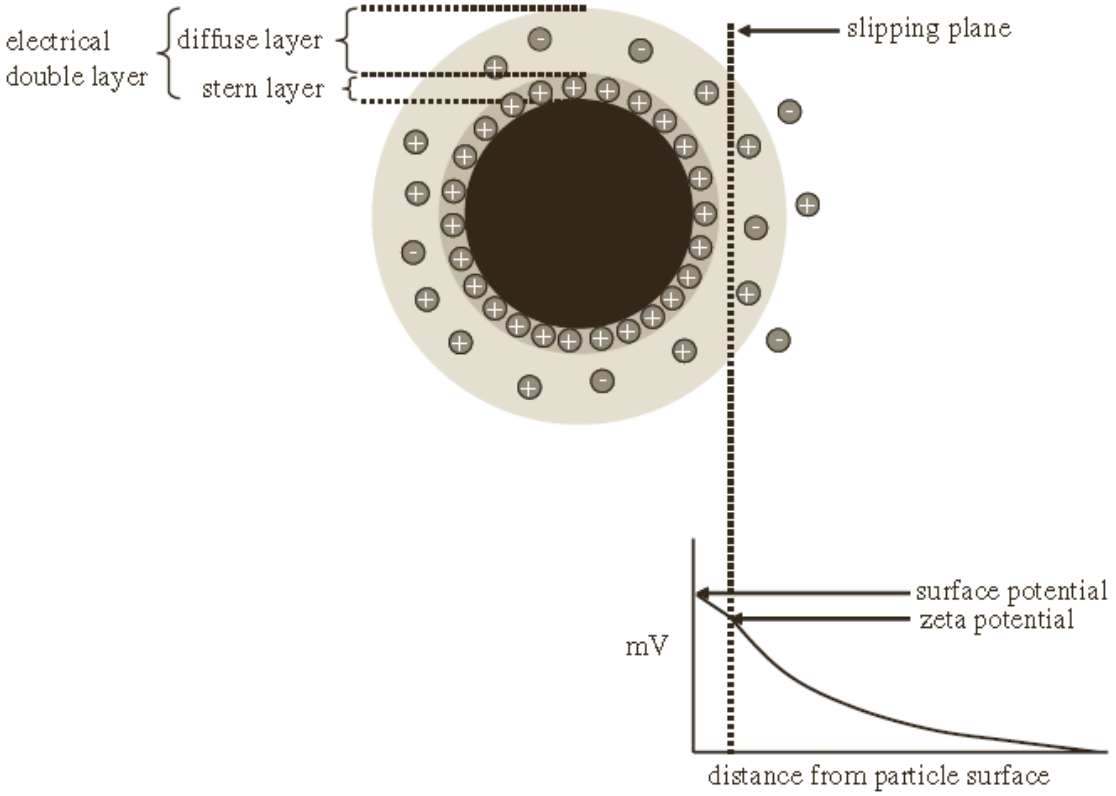

Figure 5. A particle in aqueous medium surrounded by the electric double layer. Within the diffuse layer the surface of hydrodynamic shear, or the slipping plane, contains the ions that move with the particle. The zeta potential is defined as the electric potential at the slipping plane (Kaszuba et al. 2010).

Since the zeta potential ζ cannot be measured directly, the instrument is instead used to measure the velocity V of the particles in an applied electric field E, which is then used to calculate the electrophoretic mobility μ_e (Bhattacharjee 2016):

$$\mu_e = \frac{V}{E} \tag{2}$$

The electrophoretic mobility is converted to the zeta potential by using the Helmholtz-Smoluchowski equation,

$$\mu_e = \frac{\varepsilon_r \varepsilon_0 \zeta}{\eta}, \tag{3}$$

where ε_r is the relative permittivity/dielectric constant, ε_0 the vacuum permittivity, and η the viscosity of the sample at the experimental temperature. This equation is used when the electric double layer is thin compared to the particle radius and applies to most of the pharmaceutical preparations (Kaszuba et al. 2010; Bhattacharjee 2016).

The most commonly used technique to determine the electrophoretic mobility of particles is light scattering (Kaszuba et al. 2010). Malvern Zetasizer® Nano instruments use laser Doppler electrophoresis to measure small frequency shifts in the scattered light that are proportional to the speed of the particles (Kaszuba et al. 2010; Bhattacharjee 2016). The typical measurement setup is shown in Figure 6. In this technique, the laser beam is split into two, one beam is the reference, and the other one is directed towards the sample. The Doppler shift is determined when the scattered light from the sample optically interferes with the reference beam. Since the laser beam must penetrate the sample, it must be optically clear (Kaszuba et al. 2010).

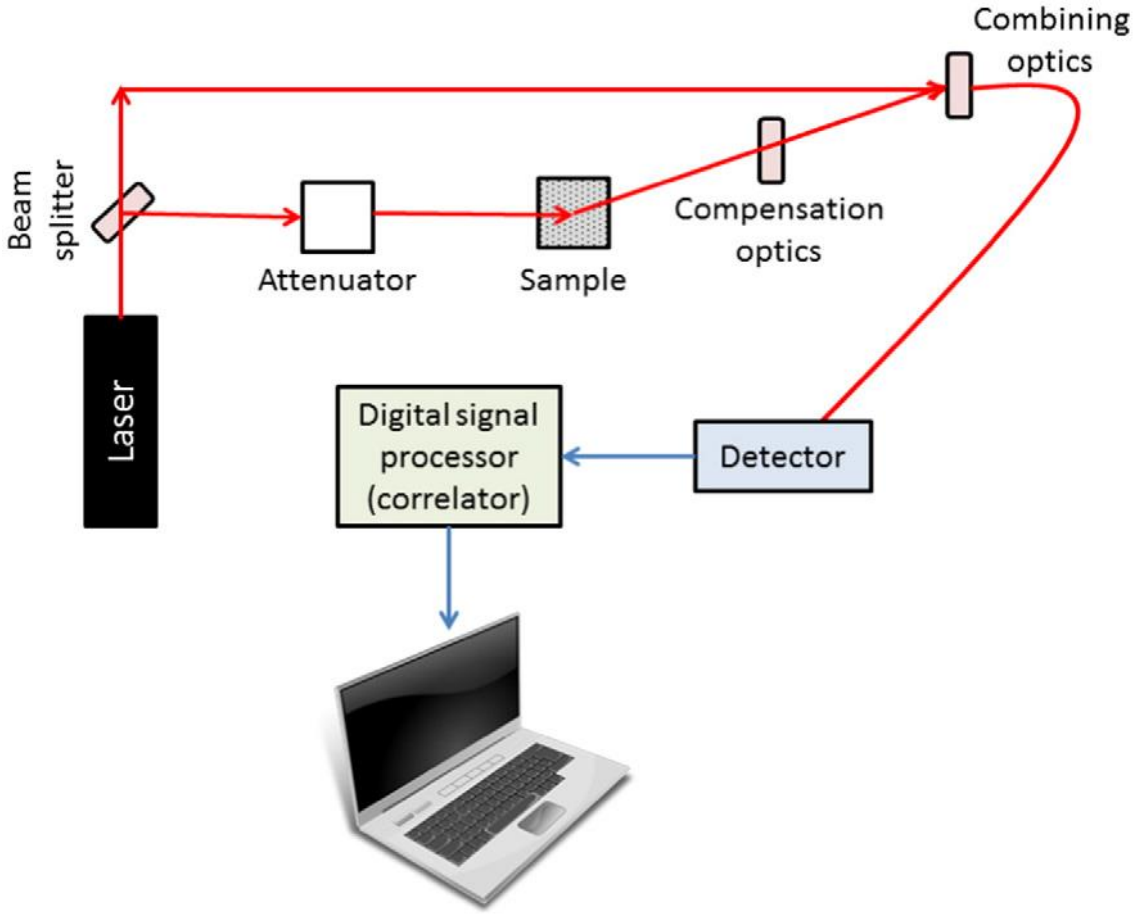

Figure 6. Schematic representation of a typical instrumentation that uses laser Doppler electrophoresis to determine the zeta potential of particles (Bhattacharjee 2016).

There are several factors that can influence the zeta potential data. One of the most influential parameter is the pH, as the zeta potential becomes more positive or negative as a result of acidic or basic pH, respectively (Uskokovic et al. 2010; Bhattacharjee 2016).

The zeta potential decreases when the EDL becomes more compressed as the ionic strength of a sample increases (Bhattacharjee 2016). The ionic strength affects the thickness of the EDL more when the sample concentration is high and therefore it also influences the zeta potential values (Kaszuba et al. 2010). Kaszuba et al. (2010) indicate that the high concentration zeta potential values are not realistic and therefore should be used only in a relative, not absolute sense. Also, the relation between the zeta potential and the particle concentration is determined by surface adsorption and the effect of the EDL (Bhattacharjee 2016). Even though low concentrations hardly correlate with therapeutically relevant doses the most common concentrations for zeta potential measurements are 50-100 µg/mL.

Zeta potential is also used to determine the surface charge of nanoparticles although it rather deals with surface potential and never measures charge or charge density (Bhattacharjee 2016). It also assumes that the dominant ions in the EDL up to the slipping plane are similar compared to the particle surface and therefore yields only indicative evidence on the nature of surface charge.

2.3.2 One-dimensional gel electrophoresis

One-dimensional gel electrophoresis, also called electrophoretic mobility shift assay, is a simple and advantageous method for determining the size, amount, purity, and isoelectric point of macromolecules (Shi and Jackowski 1998; Drabik et al. 2013). The separation of different macromolecules by electrophoresis happens when the charged molecules migrate through a gel matrix upon the application of an electric field. The electric field, the ionic strength and the viscosity of the solvent, and the temperature, hydrophobicity, shape and size of the molecules affect the constant migration rate:

$$\mu = \frac{V}{E} = \frac{Z}{6\pi\eta r}, \tag{4}$$

where µ is the electrophoretic mobility, V the migration speed, E the electric field strength, Z the total molecular charge, η the viscosity, and r the molecular radius.

One dimensional gel electrophoresis uses two main types of gels, polyacrylamide and agarose gels (Drabik et al. 2013). In general, agarose gel is used with large molecules

such as in nucleic acid separation, and polyacrylamide gel with smaller molecules like proteins, respectively (Shi and Jackowski 1998). When prepared by chemical polymerization, the polyacrylamide gel consists of monomeric acrylamide, N,N'-methylene-bisacrylamide (bisacrylamide), ammonium persulfate (APS), N,N,N′,N′-tetramethylethylenediamine (TEMED), electrophoretic buffer, and deionized water. Monomeric acrylamide and bisacrylamide form the polyacrylamide, and the polymerization is initiated by APS and TEMED. The acrylamide monomer is activated by APS that forms persulfate free radicals in water, and TEMED is used as the additional catalyst because it is capable of carrying electrons.

There are also other types of polyacrylamide gels such as sodium dodecyl sulfate polyacrylamide gel electrophoresis (SDS-PAGE), acid-urea-Triton X-100 (AUT), and riboflavin and methylene blue systems (Shi and Jackowski 1998). The rate of polymerization and the properties of the gel are affected by several factors. The initiators can either accelerate or inhibit the polymerization. Usually the methylene blue system is the fastest, then the persulfate system, and the riboflavin system is the slowest. Also in chemical polymerization, the higher the initiator concentration the faster is the polymerization. Contaminants in reagents can also affect the polymerization rate. For example, TEMED contains oxidation products and loses catalytic activity with time, and APS solution should be freshly prepared since it is very hygroscopic and decomposes when dissolved in water. Since oxygen traps free radicals, it inhibits the acrylamide polymerization, and degassing under vacuum is recommended prior to the polymerization.

Caglio and Righetti (1993) discovered in their study that pH has different effect depending on the used initiator. The APS-TEMED system gives optimum performance between pH 7–10, and no polymerization occurs at pH 4. For the riboflavin-TEMED system the optimal pH range for polymerization is between pH 4–7 with a peak about pH 6.2, and no polymerization occurs at pH 10. The methylene blue system has remarkably good performance between pH 4-8, and sufficient performance between pH 9-10. These results are important when preparing acrylamide gels.

Polyacrylamide gel electrophoresis has been used to study siRNA or dsDNA binding to cationic liposomes or different proteins (Geoghegan et al. 2012; Koide et al. 2016). A fixed amount of siRNA or dsDNA will bind itself to the cationic liposomes or different proteins. Any siRNA or dsDNA that is not or is only loosely attached to the lipoplexes or proteins will enter the gel during the electrophoresis. Instead in stable complexes the siRNA or dsDNA does not enter the gel. In the Geoghegan et al. (2012) study the non-specific binding of nucleic acid was enabled by the TAT motifs in PTD-DRBD (protein transduction domain - double-stranded RNA binding domain).

2.3.3 Isothermal titration calorimetry

Isothermal titration calorimetry (ITC) is a characterization method that is used to study biomolecular interactions (Pierce et al. 1999). It measures the thermodynamic properties of biomolecule binding. ITC can determine several reaction parameters, such as the binding constant K, reaction stoichiometry N, enthalpy ΔH and entropy ΔS, in a single experiment.

ITC is composed of two identical cells (Pierce et al. 1999). The first cell contains either water or buffer and acts as a reference, and the other one contains the sample. The cells are placed inside an adiabatic jacket, as shown in Figure 7. The jacket temperature is usually 5–10 °C lower than the temperature inside the cells. Both cells have electric heaters and temperature sensors. The injection syringe is filled with the titrated ligand, and the syringe is then placed into the sample cell. Prior to first injection the reference and sample cells are calibrated to the same temperature. The baseline of the experiment is given by a constant power (<1 mW) applied to the reference cell. During the injection of the titrant the binding reaction either absorbs or releases heat in the sample cell depending whether the reaction is endothermic or exothermic, respectively. The heaters will compensate for the resulting temperature difference between the cells, and return the cells to equal temperature, while the heat flow is measured.

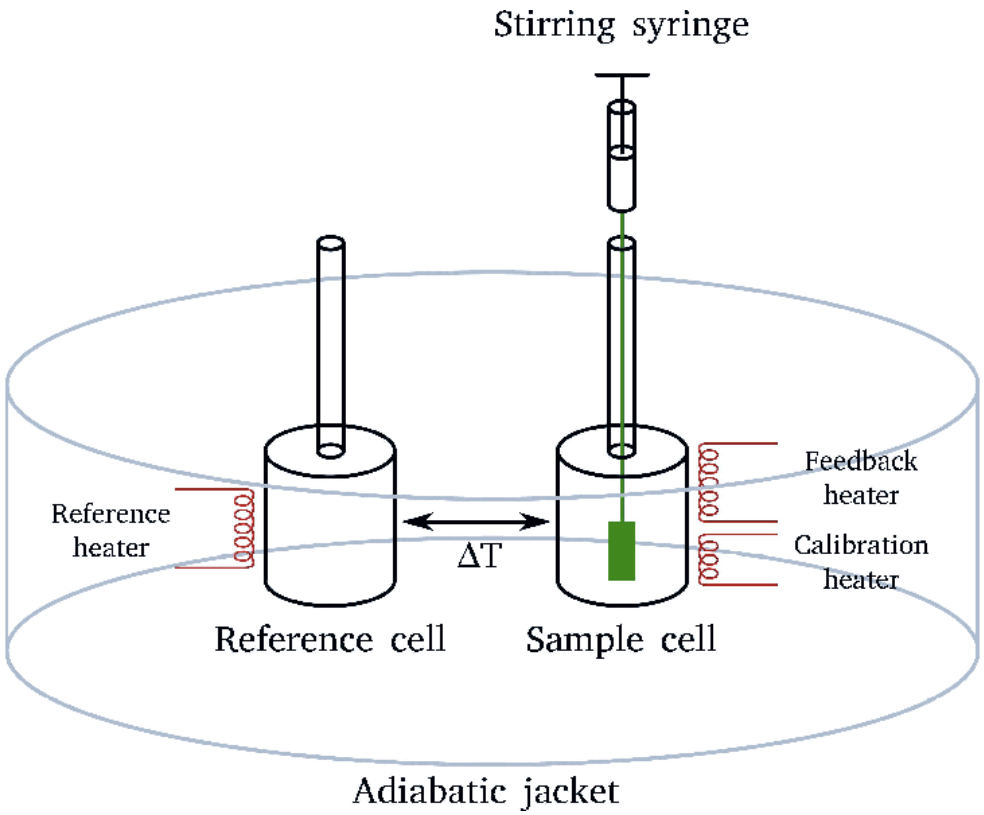

Figure 7. Schematic depiction of an isothermal titration calorimeter.

In a single-injection instrument, after the actual titration it is important to perform control experiments (Pierce et al. 1999). To determine the heat of dilution of the ligand, it is titrated identically into a sample cell containing only the buffer. The less significant control experiment determines the heat of dilution of the macromolecule where usually buffer is titrated into the sample cell filled with the macromolecule. Since ITC is very sensitive it is important to be extremely careful with all aspects of the experiment. Prior to the experiment all the solutions and samples need to be degassed under vacuum to avoid air bubbles. The initial sample concentrations are critical to accurate interaction data. Also, it is important to take into consideration the ionization enthalpy of the buffer since a large enthalpy will reflect buffer ionization and protonation. For example, the enthalpy of ionization of sodium phosphate buffer is 1 kcal/mol and of TRIS-HCl buffer 11 kcal/mol.

Several studies have used ITC to determine the interaction between DNA or RNA oligonucleotides and cationic liposomes (Kennedy et al. 2000; Pozharski and MacDonald 2002; Lobo et al. 2003; Nascimento et al. 2015). Kennedy et al. (2000), and Pozharski

and MacDonald (2002) studied the effect of ionic strength to enthalpy and liposome – DNA complex formation. They titrated cationic liposomes to a DNA solution and DNA to cationic liposomes. The buffers contained 20 mM HEPES, 0.1 mM EDTA and different amounts of NaCl. They found out that at low ionic strength the equilibrium DNA/lipid concentration ratio is higher than at high ionic strength. Pozharski and MacDonald (Pozharski and MacDonald 2002) studied also different types of cationic liposome composition, and their interaction with DNA. Nascimento et al. (2015) titrated siRNA to cationic liposomes with and without a hyaluronic acid coat.

3 AIM OF THE STUDY

This research work is aimed to develop and characterize innovative poly-cationic liposomal platforms for gene delivery, using a novel synthetic cell-penetrating enhancer. Liposomes are surface-engineered with the CPE, obtaining a cationic charged formulation that will be then exploited for dsDNA loading.

The study has three main characterization steps. The first step is to decorate liposomes with the novel CPE by post insertion to obtain preformed cationic vesicles. Increasing amounts of CPE are added to the lipidic formulation, measuring its encapsulation by zeta potential analysis: the higher the CPE ratio on the liposome surface, the more positive the zeta potential becomes. The second step involves oligonucleotide loading by a post insertion procedure. These formulation strategies are investigated in order to assess their effect on the loading capacity of the lipoplexes and to find the final formulation with the highest loading efficiency. The final step is to investigate the thermodynamics of the cationic liposome/oligonucleotide association by microcalorimetric studies.

4 MATERIALS AND METHODS

4.1 Novel cationic lipoplexes

Novel cationic lipoplexes used in the experiments consists of cationic liposomes generated with two different lipids (phospholipid and cholesterol), a post-inserted cationic synthetic lipid that is developed and synthetized in the University of Padova, and an oligonucleotide. Figure 8 represents a diagram of the lipoplexes studied in this thesis work.

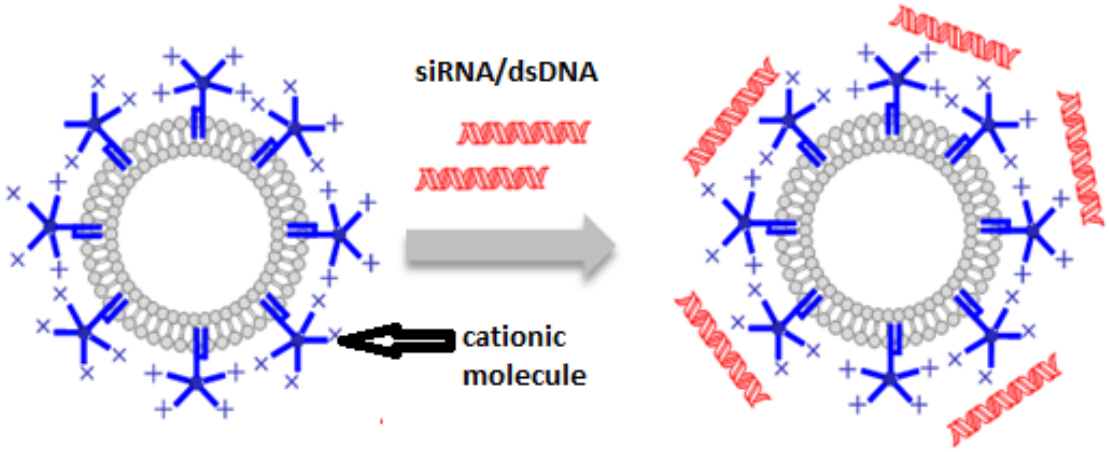

Figure 8. Diagram representing the lipoplex generated in this thesis work. In grey the lipid bilayer forms the liposome, in blue the cationic synthetic lipids are inserted into the lipid bilayer. The oligonucleotides (red) are adsorbed on the surface of the cationic liposomes. Image by Silvia Gallina, University of Padova.

- The neutral lipids used to prepare the liposomes were egg phosphatidylcholine (EggPC, Lipoid E 80) that was purchased from Lipoid AG (Steinhausen / ZG Switzerland), and cholesterol from Sigma-Aldrich (St. Louis, MO, USA). The molecular structures of the main phospholipid component in EggPC and cholesterol are shown in Figure 9 and Figure 10, respectively.

Figure 9. Molecular structure of the main phospholipid component in EggPC. (Lipoid GmbH 2016)

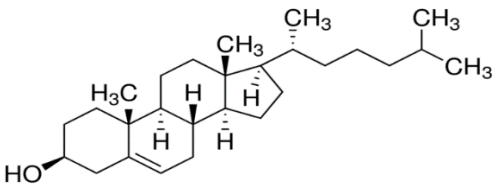

Figure 10. Molecular structure of cholesterol. (Sigma-Aldrich 2016)

- The cationic and synthetic CPE used to provide for positive charge in the liposomes is a novel non-peptidic oligo-guanidyl derivative (OGD), which was conjugated to an unsaturated alkyl chain (length 18 carbon atoms) for liposome anchoring to the lipid bilayer. A previously synthetized OGD was developed after intensive study of the TAT (trans-activator of transcription) peptide and its derivatives in the University of Padova (Bersani et al. 2012). In this study two varieties of OGD were used, one with 4 positive charges (OGD4) and the other with 6 positive charges (OGD6). The molecular weights of OGD4 and OGD6 are 2266.59 g/mol and 3925.49 g/mol, respectively. A solution of the oligo-guanidyl moiety conjugated with a lipophilic side-chain was prepared either in HEPES or TRIS buffer.
- Double stranded DNA (dsDNA) (biomers.net GmbH, Ulm, Germany) was used in this study as an oligonucleotide model to mimic small interfering RNA (siRNA). The dsDNA used contains 38 phosphate groups.

Initially another lipid, hydrogenated soy phosphatidylcholine (HSPC, PHOSPHOLIPON® 80 H, Lipoid AG), was used instead of EggPC. The HSPC (shown in Figure 11) was chosen in the beginning because a combination of HSPC and cholesterol have been used in previous studies and in several commercial formulations such as Doxil® and Ambisome® (Fan and Zhang 2013; Li et al. 2015). HSPC was

replaced with EggPC because the liposomes consisting of HSPC and cholesterol were not stable when assembled with OGD. EggPC was chosen because EggPC liposomes have proved to have a higher encapsulation efficiency and better drug carrying ability than soy phosphatidylcholine liposomes (Li et al. 2015). A commercial liposomal product Myocet® has EggPC in its lipid composition.

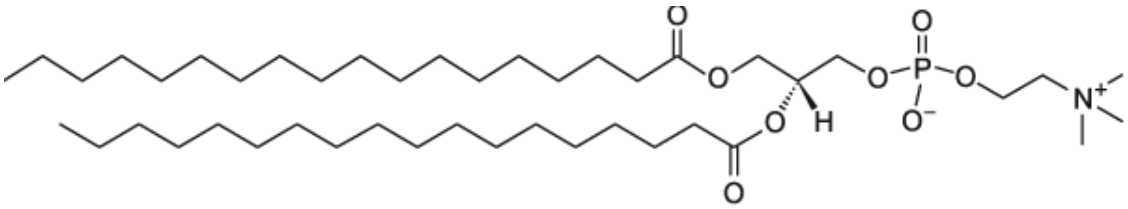

Figure 11. The molecular structure of HSPC. (Avanti Lipids Polar 2016)

4.2 Buffer preparation

All the aqueous buffer solutions were based on Milli-Q water (Merck Millipore KGaA, Darmstadt, Germany). A Seven Easy S20-K Mettler Toledo pH meter with a Mettler Toledo Inlab 413 electrode (Schwerzenbach, Switzerland) together with a Fischerbrand Hydrus600 pH meter were used to measure the pH. The pHs of the buffer solutions was adjusted by HCl and NaOH solutions. The following buffers were used in the experiments unless otherwise stated.

- The main buffer used in the experiments was a HEPES (4-(2-hydroxyethyl)-1-piperazineethanesulfonic acid) buffer solution at pH 7.4 to mimic neutral pH conditions (10 mM HEPES (Sigma-Aldrich) and 150 mM of NaCl) with isotonic osmotic pressure. The molecular structure of HEPES is shown in Figure 12.

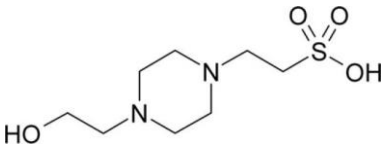

Figure 12. Molecular structure of HEPES.

- The citrate buffer was used to mimic acidic endosomal conditions at pH 5.0 (Sorkin and von Zastrow 2002). It was prepared by using 80 mM trisodium citrate dehydrate (Carlo Erba Reagents SAS, Val de Reuil, France) to create an isotonic buffer. The molecular structure of trisodium citrate dehydrate is shown in Figure

13. No NaCl was added to this buffer because the ionic strength was already sufficiently high.

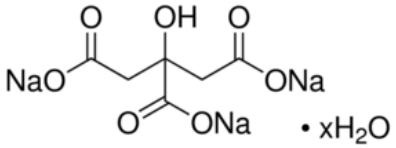

Figure 13. Molecular structure of trisodium citrate dihydrate

- TRIS buffer at pH 7.4 was used in isothermal titration calorimetry (ITC) measurements. The TRIS buffer contained 10 mM 2-Amino-2-(hydroxymethyl)-1,3-propanediol base (TRIS, Sigma-Aldrich) (structure shown in Figure 14), 1 mM ethylenediaminetetraacetic acid (EDTA, Sigma-Aldrich) and 50 mM NaCl. TRIS was chosen because it was the annealing buffer of the dsDNA.

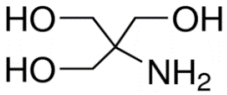

Figure 14. Molecular structure of TRIS

- A concentrated electrophoresis buffer (TBE) was prepared by using 1 M TRIS, 1 M boric acid (Merck Millipore KGaA) and 20 mM EDTA and Milli-Q water. The pH of the buffer was adjusted to 7.4. The running buffer for electrophoresis measurements was prepared by diluting the TBE buffer ten times by using deionized water.

Since the buffers affect the different characterization methods it is important to determine parameters such as ionic strength (Varenne et al. 2015). The physico-chemical properties of the buffers are presented in

Table 1 and these were calculated by using the equations below (Sinko and Singh 2011b; Sinko and Singh 2011c; Sinko and Singh 2011a). The ionic strength I is defined as

$$I = \frac{1}{2}\sum_i \frac{c_i}{c_0} {z_i}^2, \tag{5}$$

where c_i is the concentration, c_0 mol/L and z the charge of the ion in units elementary charge e, respectively (Sinko and Singh 2011b).

The buffer capacity β is given by

$$\beta = 2.3\ C\ \frac{K_a[H_3O^+]}{(K_a + [H_3O^+])^2} \tag{6}$$

and the maximum buffer capacity β_{max} is obtained when $[H_3O^+] = K_a$, i.e. when pH is equal to the acid dissociation constant pK_a, which yields

$$\beta_{max} = 0.576\ C, \tag{7}$$

where C is the total concentration of the buffer (Sinko and Singh 2011a).

The apparent acid dissociation constant pK_a' is determined by using the Debye-Hückel relationship

$$pK_a{}' = pK_a + (2\varepsilon - 1)\left[\frac{A\sqrt{I}}{1 + \sqrt{I}} - 0.1I\right], \tag{8}$$

where ε is the charge on the conjugate acid species and A the temperature dependent constant that is 0.51 at 298 K. The ionic strength of the solutions affects the acid association constant and thus the buffer capacity. Therefore, it is important to determine the pKa' and the apparent buffer capacity (apparent β) which take the ionic strength into consideration. The apparent β can be determined with Equation 6 but with K_a' used instead of K_a.

Biochemical properties of the buffers should match those of human blood as the ultimate objective is to use this method for gene delivery in humans. The osmotic pressure π of blood is 7.7 atm. It can be calculated for electrolyte solutions by using van't Hoff's formula

$$\pi = \sum_k c_k i_k RT, \tag{9}$$

where c_k is the concentration of the k^{th} salt in the solution, and i_k is the corresponding correction factor that approaches the number of ions the salt dissociates in dilute solution (Sinko and Singh 2011c).

Table 1. Significant physico-chemical parameters of HEPES, TRIS and citrate buffers. The pK_a values for HEPES and TRIS are from Sigma-Aldrich and for citrate from Carlo Erba Reagents.

	HEPES pH 7.4	TRIS pH 7.4	citrate pH 5
pK_a	7.50	8.07	4.76
pH range	6.8–8.2	7.5–9.0	3.0–6.2
Buffer salt concentration (mol/L)	0.01	0.01	0.08
Maximum buffer capacity β_{max}	0.0058	0.0058	0.0461
NaCl concentration (mol/L)	0.15	0.05	0
EDTA concentration (mol/L)	0	0.001	0
Ion strength I	0.160	0.068	0.480
Apparent pK_a'	7.37	8.17	4.60
β at chosen pH	0.0057	0.0033	0.0427
Apparent β	0.0057	0.0029	0.0374
Osmotic pressure (atm)	7.829	3.034	7.829
Suggested working concentration (mol/L) (Sigma-Aldrich)	0.01–1	0.01–0.0625	–

4.3 Liposome preparation and different characterization methods

The lipid stock solutions were obtained by dissolving the lipids in a mixture of chloroform and methanol (Sigma-Aldrich). The concentrations of the lipid solutions were 6.45 mg/mL and the molar ratio of chloroform and methanol was 1:2. The phospholipid-cholesterol mixture was prepared by mixing the stock solutions of lipids in a round bottom flask with a 2:1 EggPC/cholesterol molar ratio. The solvents methanol and chloroform were then evaporated by using a vacuum rotary evaporator system (Büchi R-114, Büchi Labortechnik AG, Flawil, Switzerland) at 25–30 °C, so that a thin lipid film was formed on the wall of the flask. To ensure that all the organic solvents were evaporated the flask was placed into a desiccator which was attached to a vacuum pump (Büchi Vac V-500) for at least 4–5 hours.

The lipid layer was re-hydrated in 200–400 µL of buffer solution and vortexed. Then the liposomes were subjected to freeze-thaw cycles prior to extrusion to obtain monodisperse particle profiles (Castile and Taylor 1999). The freezing was done in liquid nitrogen and the thawing in glycerol at 65 °C, and the cycle was repeated 10 times. After the freeze-thawing cycles buffer was added to form a solution with a lipid concentration of 20

mg/mL (16 mg/mL of EggPC and 4 mg/mL of cholesterol). The liposome solution was then sonicated in an ultrasonic bath (Power Sonic410, Hwashin Technology CO, Seoul, Korea) for 10 minutes at 37 °C to further narrow down the particle size distribution. Then the liposomes were extruded 11 times with a 200 nm cut-off filter by using an Avanti Polar mini-extruder (Alabaster, AL, USA). The same procedure was used with all three buffers. This whole procedure is shown and explained in Figure 15.

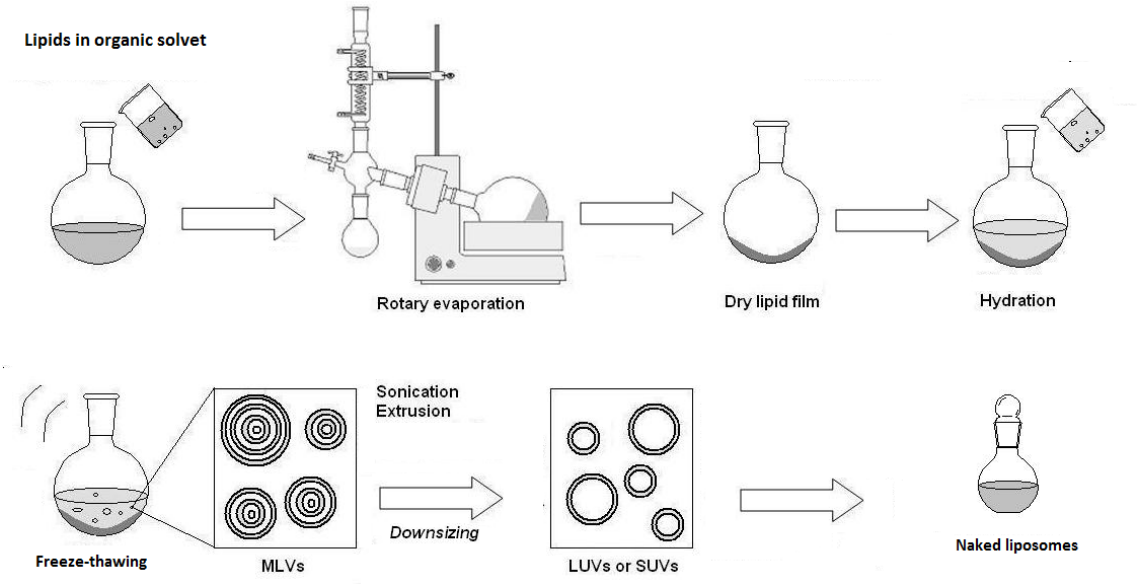

Figure 15. Schematic depiction of liposome preparation from lipid stock solutions (Lopes et al. 2013, p. 95).

4.3.1 Post-insertion of oligo-guanidyl derivative

An oligo-guanidyl derivative solution was prepared by dissolving 3 mg/mL of OGD powder in buffer solution. Since OGD was not soluble at pH 5 it was solubilized at pH 7.4, by using either the TRIS or HEPES buffer. The solution was sonicated by using a probe-type sonicator (Omni-Ruptor 250, Ultrasonic homogenizer, Omni Inc., Kennesaw GA, USA) for 15 minutes. The appropriate amount (see below) of OGD solution was added to 150–250 µL of extruded liposomes (20 mg/mL). The liposome/OGD mixture was vortexed after each 200 µL of added OGD. The total amount of OGD was 392-654 µL and 317-529 µL for OGD4 and OGD6, respectively, to obtain different mol-%. The final cationic liposome concentration of 3–5 mg/mL was reached by adding a suitable volume of either HEPES, TRIS or citrate buffer.

4.3.2 Post-insertion of double stranded DNA

After determining the best mol-% of OGD to create cationic liposomes, different amounts of dsDNA were added to the optimized cationic liposomes to assess the maximum amount of dsDNA that binds to them as a proxy for dsDNA loading. The dsDNA was added to the diluted cationic liposomes and the samples were vortexed and maintained at room temperature for 30 minutes to promote the dsDNA association with the cationic liposomes. Different nitrogen/phosphate (N/P) ratios were prepared by adding increasing amounts of 10 µM or 100 µM dsDNA solution to 20 µL of cationic liposomes containing 17 nmol of OGD4 or 8.08 nmol of OGD6. "N" represents the cationic nitrogen in the guanidinium groups of the OGDs while "P" represent the phosphate groups in the dsDNA macromolecule. The amount of dsDNA that was added to the liposomes was calculated by using the following equation:

$$\frac{n_{ODG}}{E \times \frac{N}{P}} = n_{dsDNA}, \tag{10}$$

where E is the ratio of the positive charges in the OGD and the negative charges in the dsDNA. Since the dsDNA possesses 38 negative charges (19 base pairs) and the OGD has either 4 or 6 positive charges, E was either 9.5 (OGD4) or 6.33 (OGD6), respectively. The cationic liposome lipid concentration in the sample was diluted to 0.1 mg/mL by using the buffer that was used to prepare the liposomes. The dsDNA association measurements were performed in 10 mM HEPES (pH 7.4), 10 mM TRIS (pH 7.4), and 80 mM citrate (pH 5.0) buffers.

4.3.2 Size and zeta potential measurements with dynamic light scattering

The size and zeta potential of the cationic liposomes were measured by dynamic light scattering (DLS) by using a Zetasizer NanoZS instrument (Malvern Instruments, Malvern, Worcestershire, UK). Disposable cuvettes were used for size measurements (ZEN0010, Malvern) and for zeta potential measurements (either DTS1070 or DTS1060/DTS1061, Malvern).

The DLS measurements were performed at 25 °C. When size measurement was performed, the equilibration time was 120 seconds, the scattering angle was 173° and 5 measurements per sample were carried out. The number of runs was on automatic setting and the delay between measurements was 5 seconds.

The zeta potential measurements were analyzed according to the Smoluchowski model and the equilibration time was set to 120 seconds. The duration of each measurement was automatic from 10 to 100 runs, 3 measurements were always recorded from one sample and the delay time was set to 0 seconds.

The size and zeta potential measurements were first performed in HEPES buffer (pH 7.4) on cationic liposomes formulated with different amount of OGD. For these measurements, the concentration of the naked liposomes was always either 0.5 (OGD4) or 1 (OGD6) mg/mL. The OGD percentage (of the total liposome mass) was 8–15.5 % for OGD4, and 2.5–10 % for OGD6, depending on the sample. The goal of the measurements was to identify the best ODG percentage on liposomes that yields a suitable size and zeta potential before adding the dsDNA for post insertion.

After these measurements, the aim was to find out the highest stable N/P ratio by adding different amounts of dsDNA solution to the cationic liposomes. A 0.1 mg/mL liposome concentration was used for dsDNA association studies.

The lipoplex stability was measured by DLS for 14.5 hours at 37 °C by measuring the size every half an hour. The colloidal stability study was repeated 3 times with HEPES buffer and 3 times with 15 % of fetal bovine serum (FBS) added to the HEPES buffer samples.

4.3.3 Electrophoretic mobility shift assay

The gel electrophoresis experiments were used to assess the affinity of dsDNA with the cationic liposomes. The experiments were performed with cationic liposomes at pH 7.4 by using a 10 mM TRIS buffer, and at pH 5.0 in an 80 mM citrate buffer. The gel running

buffer at pH 7.4 was TBE as described earlier. The cationic liposomes were prepared as explained above with either 10 % or 5 % of OGD4 or OGD6, respectively, of the total lipid content. The different N/P ratios were obtained by using 10 µL of cationic liposomes further diluted to the required concentrations and by adding either 2.58 µL (OGD4 samples) of a solution containing 300 ng (corresponding to 2.58×10^{-11} mol) of dsDNA or 2.68 µL (OGD6 samples) of a solution containing 311 ng (2.68×10^{-11} mol) of dsDNA. The N/P ratios for OGD4 and OGD6 decorated liposomes were from 1:1.0, to 1:12, and from 1:0.5 to 1:10, respectively. The OGD4 and OGD6 concentrations in 10 µL of liposome dispersions were 0.056–1.11 mg/mL and 0.032-0.65 mg/mL, respectively. The cationic liposome concentrations were 0.14–1.7 mg/mL and 0.10-2.0 mg/mL for OGD4 and OGD6 liposomes, respectively. The amount of OGDs in cationic liposomes was calculated with Equation 10.

10 mL of a polyacrylamide gel was prepared at 12 w/v % concentration of acrylamide monomer from 4 mL of 30 w/v % acrylamide/bisacrylamide (29:1) in water solution, 2.5 mL of 0.1 M TBE and 2 mM EDTA buffer pH 7.4, 0.1 mL of 10 w/v % ammonium persulfate (APS) in water, 4 µL of N,N,N′,N′-tetramethylethylenediamine (TEMED, 0.775 g/mL) and 3.4 mL of deionized water. The APS and TEMED were used as polymerization agents of the gel. The gel electrophoresis assay was also performed at pH 5.0 by using the 80 mM citrate buffer instead of the TBE buffer.

Nine of the ten polyacrylamide gel wells received 15.08 µL of the different samples. Each sample contained 2.5 µL bromophenol blue. The wells were always filled in the same order. The first well was left empty. In the OGD4 electrophoretic assay the second well received the ladder (GeneOn GmbH, Germany). The third well received the positive control containing 2.58 µL of dsDNA and 10 µL of either TRIS buffer with pH 7.4 or citrate buffer with pH 5.0. The fourth well received the negative control containing 2.58 µL of buffer and 10 µL of cationic lipids with 5 mg/mL and 1.96 mg/mL of liposomes and OGD4, respectively. The remaining wells received lipoplexes with different N/P ratios. In the OGD6 electrophoretic assay the dsDNA volume was always 2.68 µL, and the second well received the positive control, third well the negative control (10 µL liposomes and 2.68 µL buffer), and the following 6 wells received lipoplexes with

different N/P ratios. In the positive control the concentration of OGD6 was 1.59 mg/mL in 5 mg/mL of liposomes. The gel electrophoresis was performed with an Amersham Biosciences miniVE Electrophoresis and Electrotransfer Unit system (GE Healthcare; Milan, Italy). In the OGD4 electrophoretic assay the gel was run for either 2 hours at 100 mV at pH 7.4 or 1.25 hours at pH 5.0. In the OGD6 electrophoretic assay the gels run for 1 hour. Afterwards the gel was placed for 20 minutes in a staining medium containing the DNA intercalating agent Gel Red® 10000× that was diluted 3300 times with milli-Q water to make a 3× staining solution. The gel images were obtained with the UV transilluminator ChemiDoc™ XRS + imaging system with Image Lab™ image acquisition and analysis software (Bio-Rad Laboratories, Headquarters, CA).

4.3.4 Isothermal titration calorimetry

Isothermal titration calorimetry (ITC) was used to study the thermodynamics of the interaction between the dsDNA and the cationic liposomes in TRIS buffer. The measurements were performed by using a Malvern MicroCal, LLC VP-ITC microcalorimeter system (Worcestershire, UK).

In the preliminary attempts, dsDNA concentration in the syringe was set at 20 µM. The starting concentration of OGD4 in the sample cell was 0.612 mg/mL corresponding to 270 µM, the injection volume was 10 µL and 25 injections were performed. The interval between the injections was 300 s. In a second attempt the interval was kept the same, the concentration of OGD4 was decreased to 0.490 mg/mL (216 µM) and the injection volume to 5 µL, with 52 injections. After that the injection volume was further increased to 8 µL and the interval between the injections to 350 s. The results of these attempts were not satisfactory because the OGD4 concentrations were too high and the reaction did not reach the saturation. Based on these preliminary attempts the final settings for the measurements reported below were selected.

- A volume of 280 µL of 20 µM dsDNA solution was placed in a titration syringe. The 1.5 mL sample cell was filled with 0.62 mg/mL of cationic liposomes with an OGD4 concentration of 0.245 mg/mL corresponding to 108 µM. The 1.5 mL reference cell was filled with the same buffer that was used to prepare the samples.

- The second measurement was a control made with dsDNA to measure the interaction of the dsDNA and the buffer. The sample cell was filled with the same buffer as the reference cell and the same amount of dsDNA solution was placed into the syringe.
- The third measurement was a control made with naked liposome to assess thermodynamic contribution of diluting naked liposomes with buffer. For this measurement, the reference and sample cells were filled with the buffer. The syringe was loaded with 280 µL of naked liposome with a concentration of 0.62 mg/mL corresponding to 0.97 mM.

The sample cell temperature was set to 25 °C, the stirring speed was 351 rpm, and the interval between the injections was 400 s. One measurement included 32 injections which lasted 10 seconds each. Each injection contained 8 µL of either dsDNA solution or naked liposomes.

The final ITC settings were also used with two HEPES buffers containing 10 mM HEPES and different amount of NaCl, i.e. 150 mM or 50 mM. However, these results were not satisfactory and only the ITC measurements performed with TRIS buffer are discussed in this thesis.

5 RESULTS

5.1 Dynamic light scattering results for OGD4

First the size and zeta potential of liposomes that contain different amounts of oligo-guanidyl derivatives were measured. The purpose of these measurements was to find the lowest OGD4 molar ratio that results in a sufficient zeta potential to encourage the attachment of dsDNA to the lipoplex, and a low polydispersity index (PDI) to obtain a narrow particle size distribution. The results shown in Table 2 and Figure 16 were gathered together with Anna Balasso from University of Padova. The samples with a total lipid concentration of 0.5 mg/mL were prepared in HEPES buffer at pH 7.4. The size distribution results are based on the intensity instead of Z-average because the PDI of

some samples was higher than 0.3, and therefore the average distribution of intensity, volume and number measurements would not be accurate (NanoComposix 2015). From these results the mol-% of OGD4 in liposomes for further studies was chosen to be 10 % because this sample had the lowest PDI range, a sufficiently small particle size, and a suitably high zeta potential.

Table 2. Size, zeta potential, and polydispersity index (PDI) for liposomes with different mol-% of post-inserted OGD4. The measurements were made in HEPES buffer at pH 7.4 and the total lipid concentration of the sample was 0.5 mg/mL. Results obtained together with Anna Balasso, University of Padova.

Percentage of OGD4	PDI	Size (nm)	Zeta potential (mV)
0.00 %	0.21	186.07 ±4.87	0.58 ±2.37
8.00 %	0.40	164.53 ±1.46	12.37 ±0.51
10.00 %	0.33	172.77 ±6.62	14.17 ±0.93
12.00 %	0.37	163.77 ±38.49	17.70 ±0.90
13.00 %	0.35	185.80 ±7.15	18.30 ±0.95
15.50 %	0.35	232.63 ±63.06	18.30 ±0.92

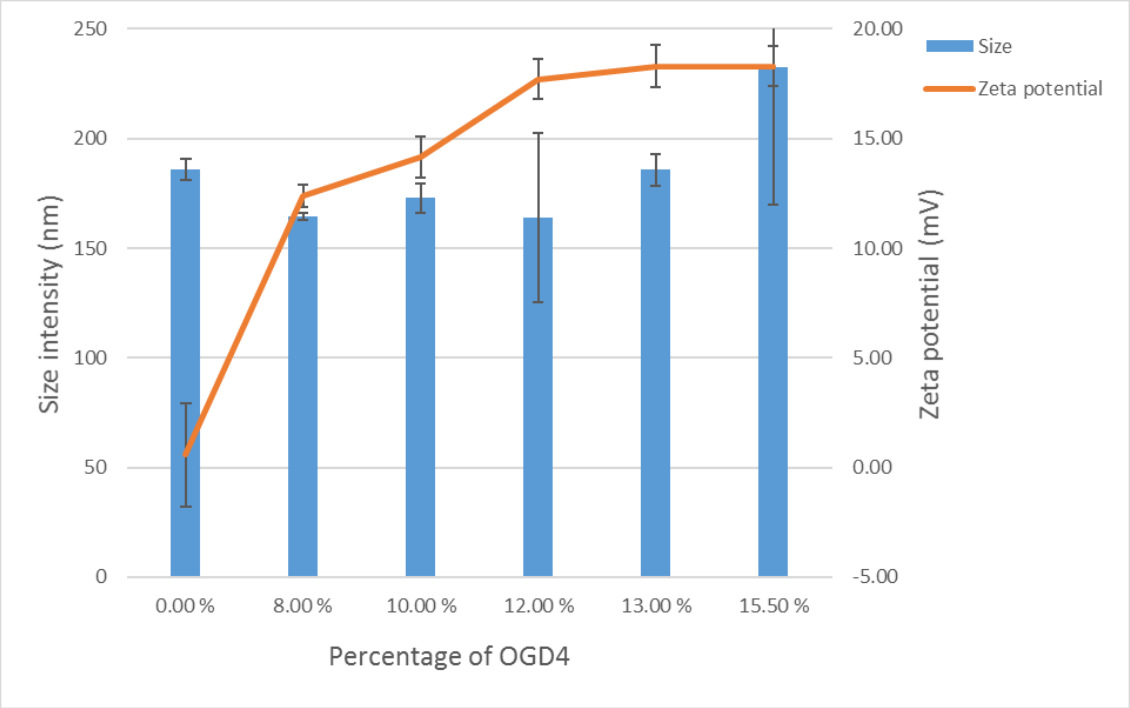

Figure 16. Size and zeta potential for liposomes with different mol-% of OGD4. The measurements were made in HEPES buffer at pH 7.4 and the total lipid concentration of the sample was 0.5 mg/mL. The bars show the size of the liposomes and the line represents the zeta potential values. Results obtained together with Anna Balasso, University of Padova.

Figure 17 shows the size results of the cationic OGD4 liposomes containing different amounts of dsDNA. Figure 18 shows the corresponding PDI values. The dsDNA complexed with cationic liposomes as soon as it was added to them. The results were measured in different buffers: HEPES and TRIS at pH 7.4, and citrate at pH 5. The total lipid concentration of the sample was 0.1 mg/mL. The nitrogen/phosphate ratio (N/P ratio) of the liposome formulation is equal to the ratio between the total positive charge from the oligo-guanidyl derivatives and the total negative charge from the dsDNA. When liposomes are plain there is no dsDNA and the amount of dsDNA increases when the N/P ratio decreases. Figure 19 shows the zeta potential results of lipoplexes with different N/P ratios. These measurements were performed only in HEPES and TRIS buffers at pH 7.4. In the TRIS buffer the size and zeta potential were also measured at N/P ratio 2, where the size was 867.16 ± 541.04 nm and the zeta potential 19.23 ± 0.86 mV. It can be seen that all the positive charges were compensated when the N/P ratio was between 5–7.5 in HEPES buffer and 1–4 in TRIS buffer, as this is where the zeta potential approaches zero.

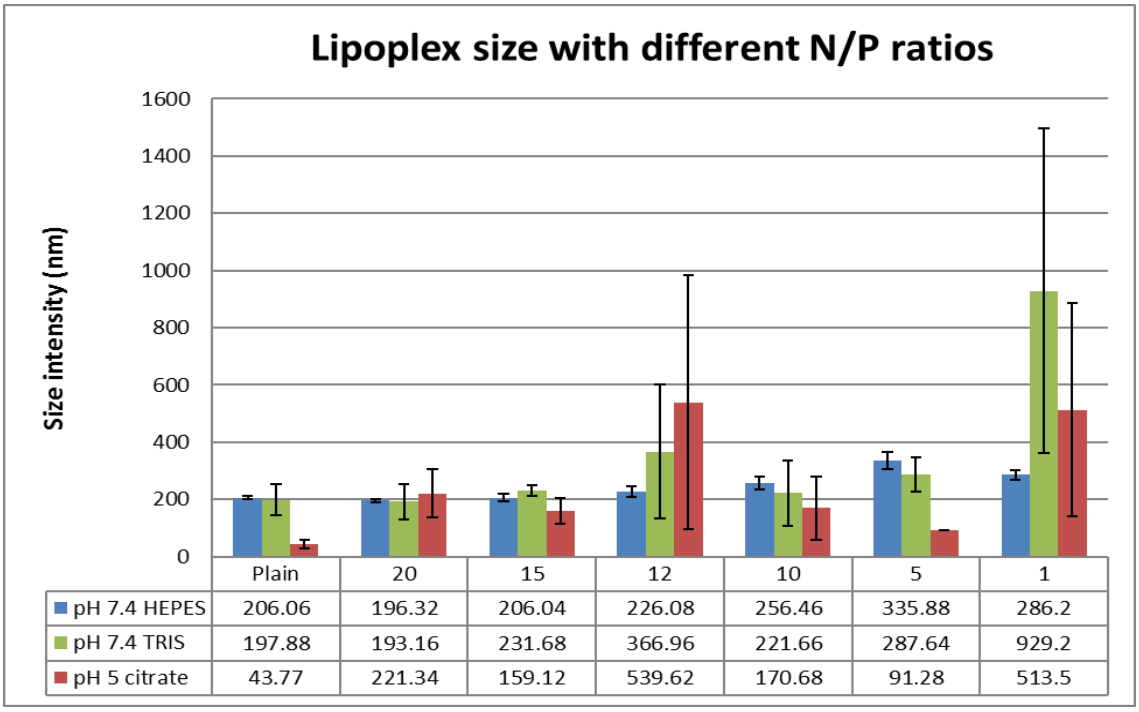

	Plain	20	15	12	10	5	1
pH 7.4 HEPES	206.06	196.32	206.04	226.08	256.46	335.88	286.2
pH 7.4 TRIS	197.88	193.16	231.68	366.96	221.66	287.64	929.2
pH 5 citrate	43.77	221.34	159.12	539.62	170.68	91.28	513.5

Figure 17. The size of the lipoplexes in different buffers. The figure shows the size versus N/P ratio. The total lipid concentration of the sample lipids was 0.1 mg/mL. The amount of the dsDNA is increasing as the N/P ratio decreases. The plain liposomes do not contain any dsDNA. Lipoplexes in HEPES buffer pH 7.4 (blue bars), TRIS buffer pH 7.4 (green bars) and citrate buffer pH 5 (red bars).

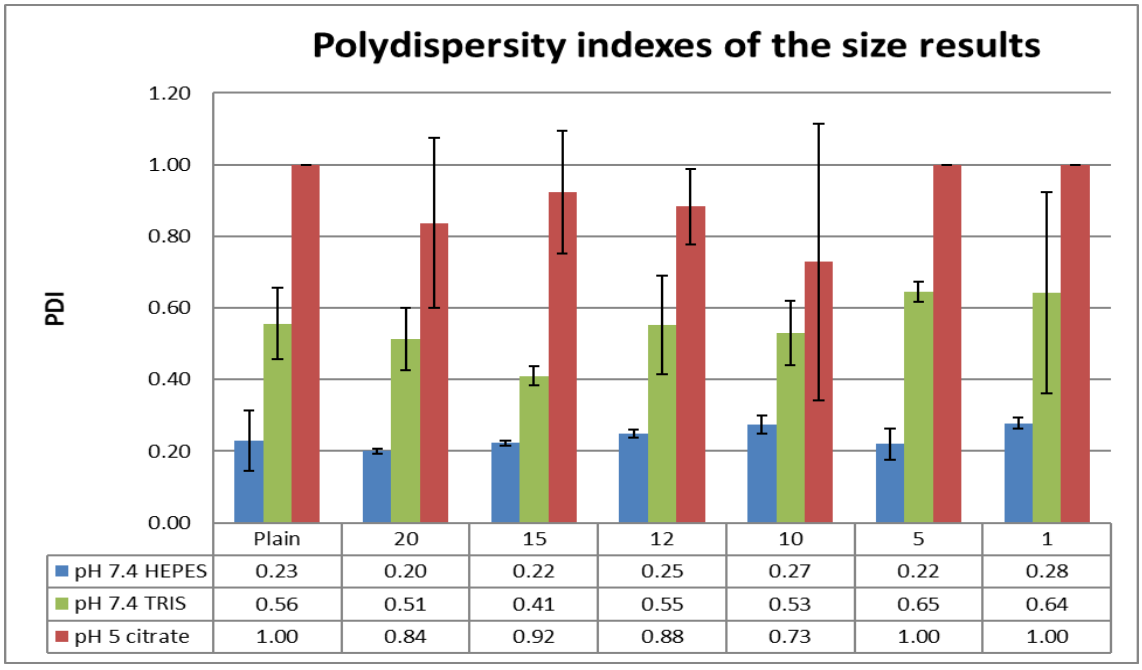

	Plain	20	15	12	10	5	1
pH 7.4 HEPES	0.23	0.20	0.22	0.25	0.27	0.22	0.28
pH 7.4 TRIS	0.56	0.51	0.41	0.55	0.53	0.65	0.64
pH 5 citrate	1.00	0.84	0.92	0.88	0.73	1.00	1.00

Figure 18. The polydispersity index of the size results. Each N/P ratio has the PDI results for lipoplexes in HEPES buffer pH 7.4 (blue bars), TRIS buffer pH 7.4 (green bars) and citrate buffer pH 5 (red bars). The total lipid concentration of the sample was 0.1 mg/mL. The amount of the dsDNA is increasing as the N/P ratio decreases. The plain liposomes do not contain any dsDNA.

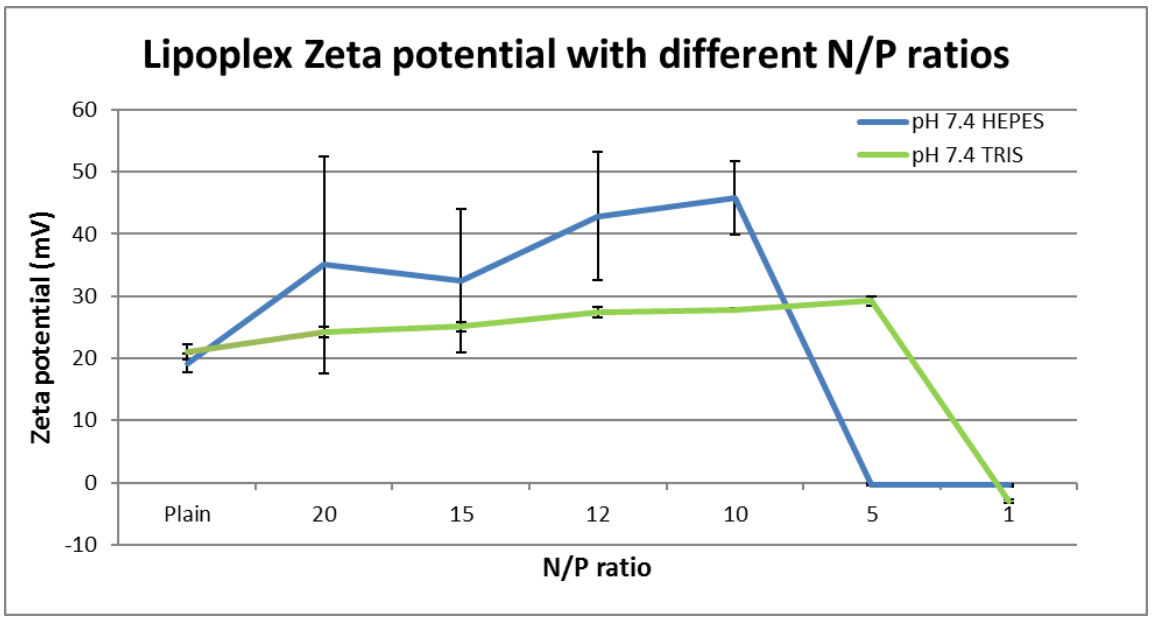

Figure 19. Lipoplex zeta potential in HEPES buffer (blue line) and TRIS buffer (green line). The total lipid concentration of the sample was 0.1 mg/mL. The amount of the dsDNA is increasing as the N/P ratio decreases. The plain liposomes do not contain any dsDNA.

Figure 20 shows the result of the stability experiment where the lipoplex size was tracked as a function of time. The buffer used in this experiment was HEPES (pH 7.4), the N/P ratio was 10, the total lipid concentration of the sample was 0.1 mg/mL, and the temperature was 37 °C. Under these conditions the lipoplexes were found to be stable. The experiments were then repeated with 15 % of FBS added to the suspension. The 15 % of FBS is the usual amount used in cell media. As can be seen from the results shown in Figure 21, in this case the lipoplexes were no longer stable. Both stability experiments were repeated 3 times and the results show the average value and standard deviation of each time point.

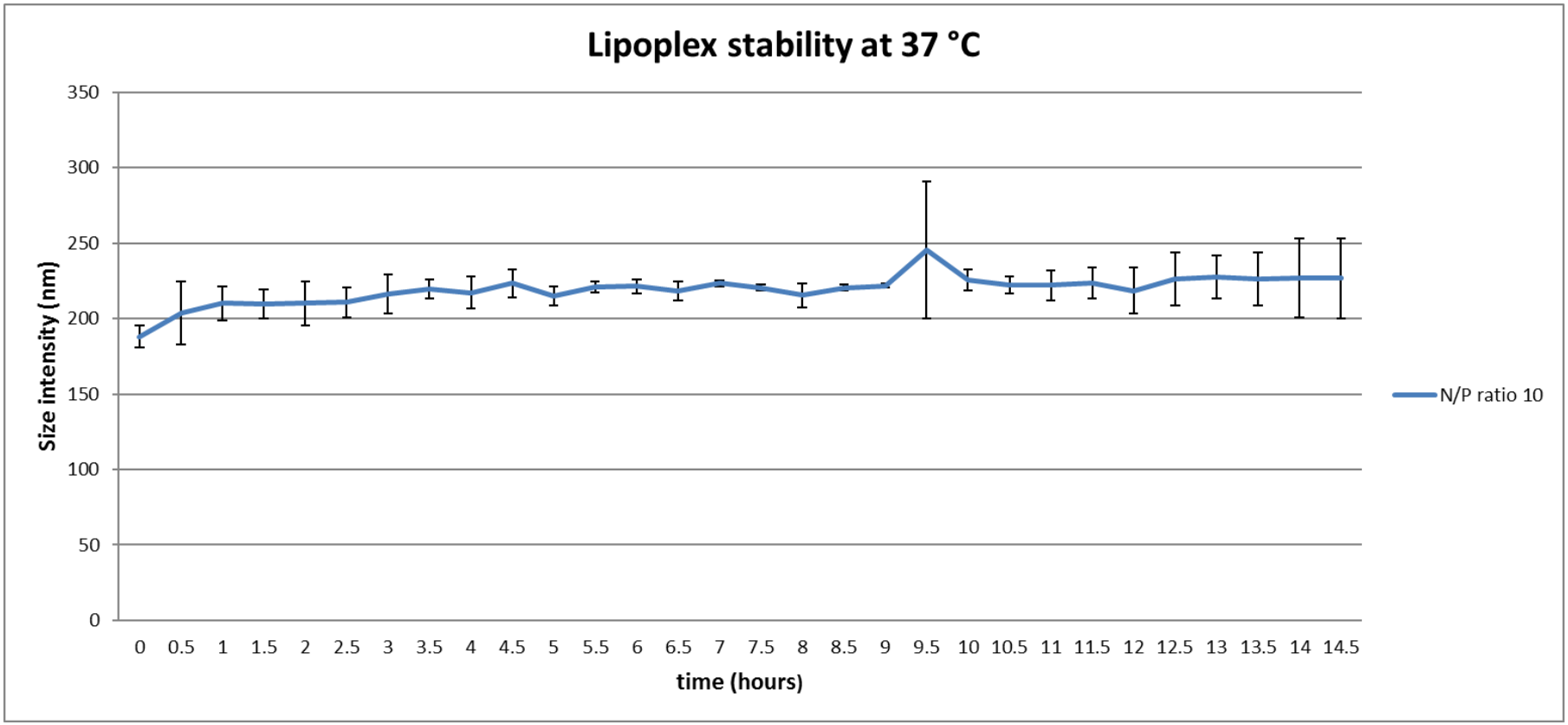

Figure 20. Lipoplex stability at 37 °C (N = 3). The measurements were recorded every half an hour for 14.5 hours. They were made in HEPES buffer, with an N/P ratio of 10, and a total lipid concentration of 0.1 mg/mL.

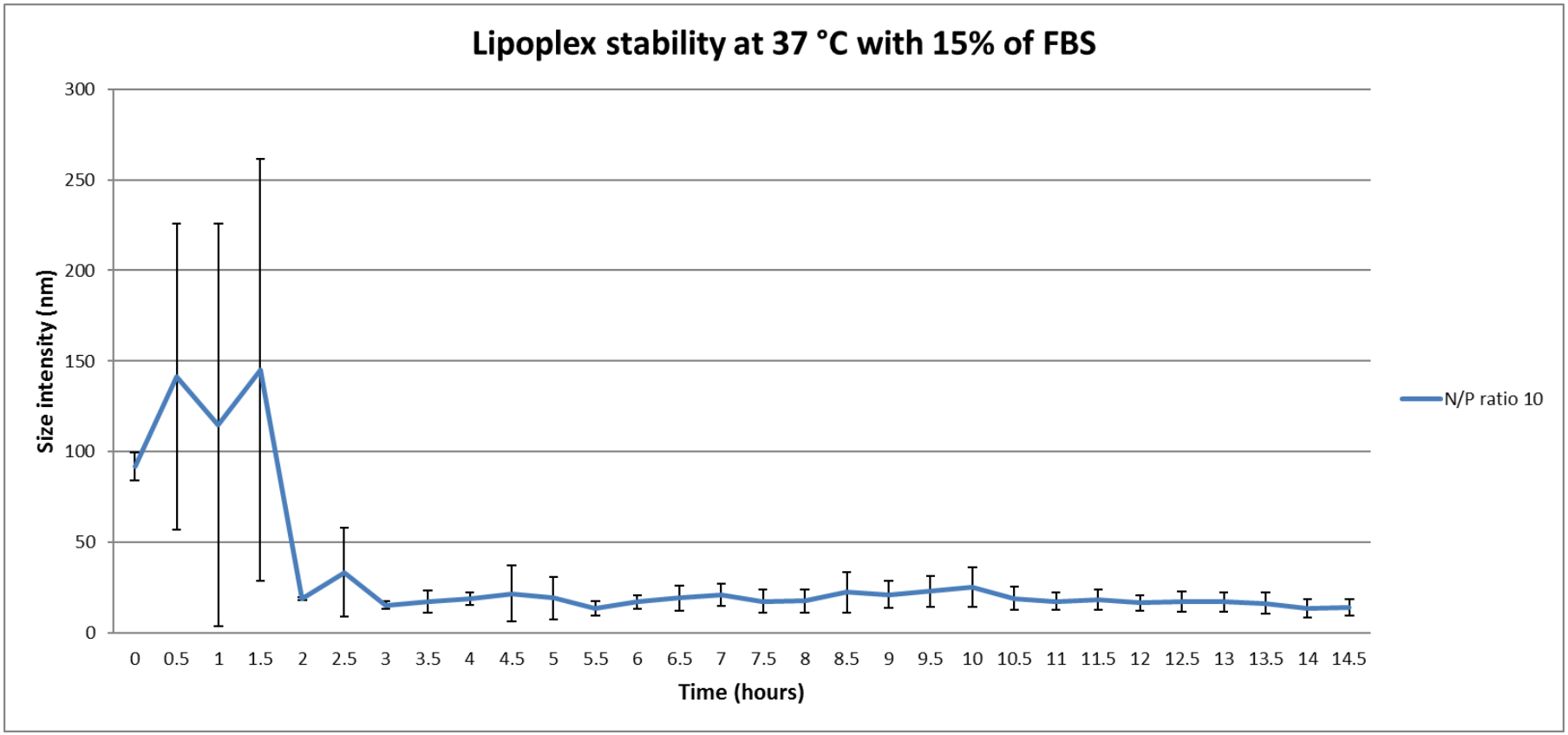

Figure 21. Lipoplex stability at 37 °C with 15 % of FBS (N = 3). The measurements were taken every half an hour for 14.5 hours. They were made in HEPES buffer, with an N/P ratio of 10, a total lipid concentration of 0.1 mg/mL.

5.2 Electrophoretic mobility shift assay for OGD4

Two electrophoretic mobility shift assays were performed, one (gel A) at pH 7.4 using the TBE buffer to run the electrophoresis, and the other (gel B) at pH 5.0 using 80 mM citrate buffer. The liposomes were prepared in 10 mM TRIS buffer (pH 7.4) or 80 mM citrate buffer (pH 5.0), respectively. Figure 22 shows the electrophoretic profiles of the gels. At pH 7.4 one can see that there was some free dsDNA remaining when the N/P ratio was smaller than 3, and all the dsDNA was attached to the OGD on the liposome surface when the N/P ratio was 5 or greater. At pH 5 the profile is very similar except that there is no free dsDNA remaining when the N/P ratio was 3 or greater. This means that more dsDNA was needed to compensate all the cationic charges in the citrate buffer with pH 5.

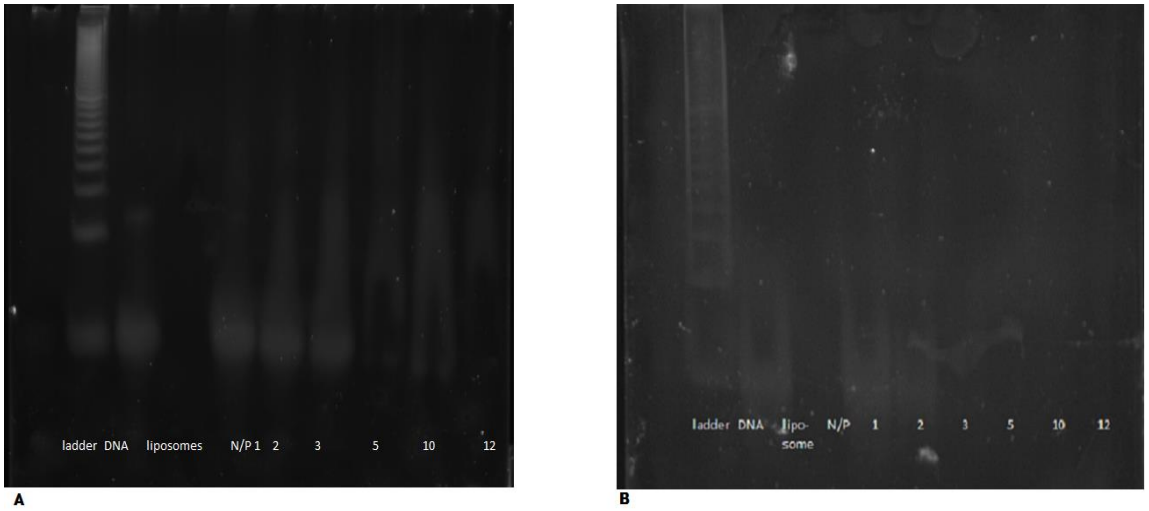

Figure 22. Electrophoretic mobility profiles of dsDNA mixed with OGD4-coated liposomes (A) at pH 7.4 and (B) at pH 5.

5.3 Isothermal titration calorimetry for OGD4

The dsDNA and cationic liposome interaction thermodynamics were measured by using isothermal titration calorimetry (ITC), in which dsDNA was titrated into cationic liposomes. The measurement temperature was 298 K (25 °C). Figure 23 shows the raw ITC data that was processed and fitted by using the AFFINImeter software (Santiago de

Compostela, Spain) to obtain the thermodynamic parameters of the interaction between dsDNA and OGD4 liposomes. Figure 24 represents the resulting ITC profile. The cumulative heat curve was plotted against the dsDNA/OGD4 molar ratio. Figure 25 shows the ITC profiles of (A) dsDNA and (B) naked liposomes titrated into the buffer. There is no noticeable interaction between the counter ions of the buffer and either the dsDNA or the naked liposomes. We therefore can conclude that the buffer and the naked liposomes did not significantly influence the thermodynamics of the dsDNA – OGD4 interaction.

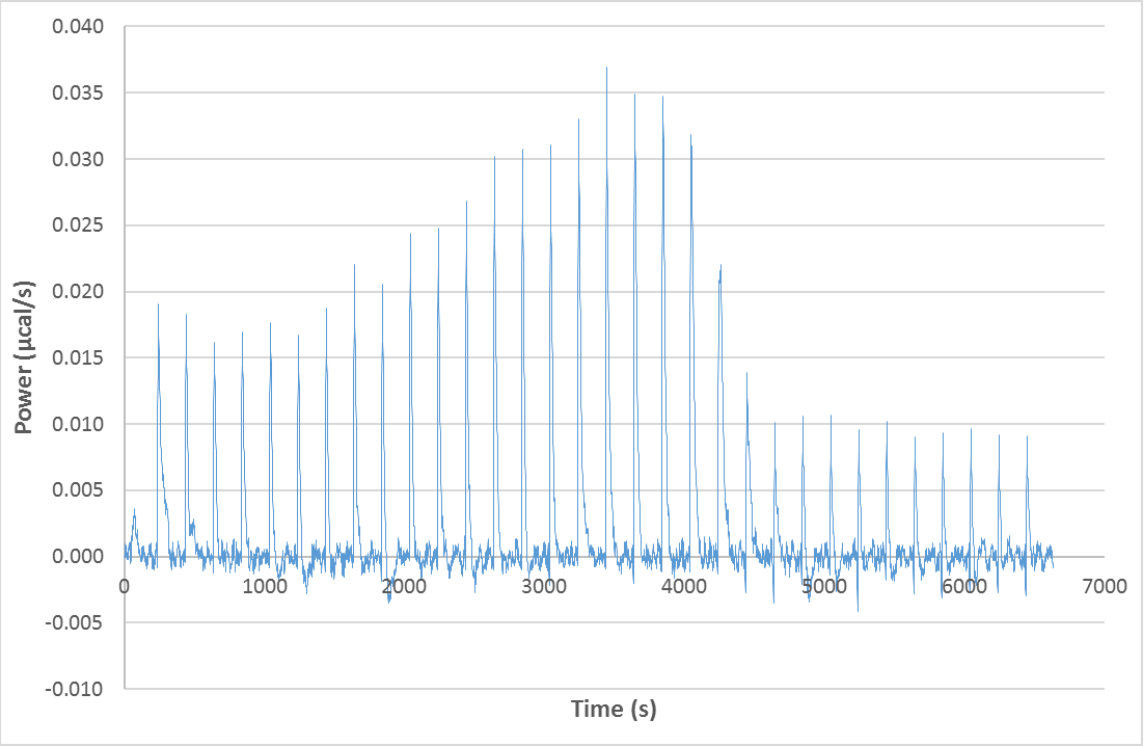

Figure 23. The raw ITC data that was processed and fitted to obtain the thermodynamic parameters of the interaction between dsDNA and OGD4 liposomes.

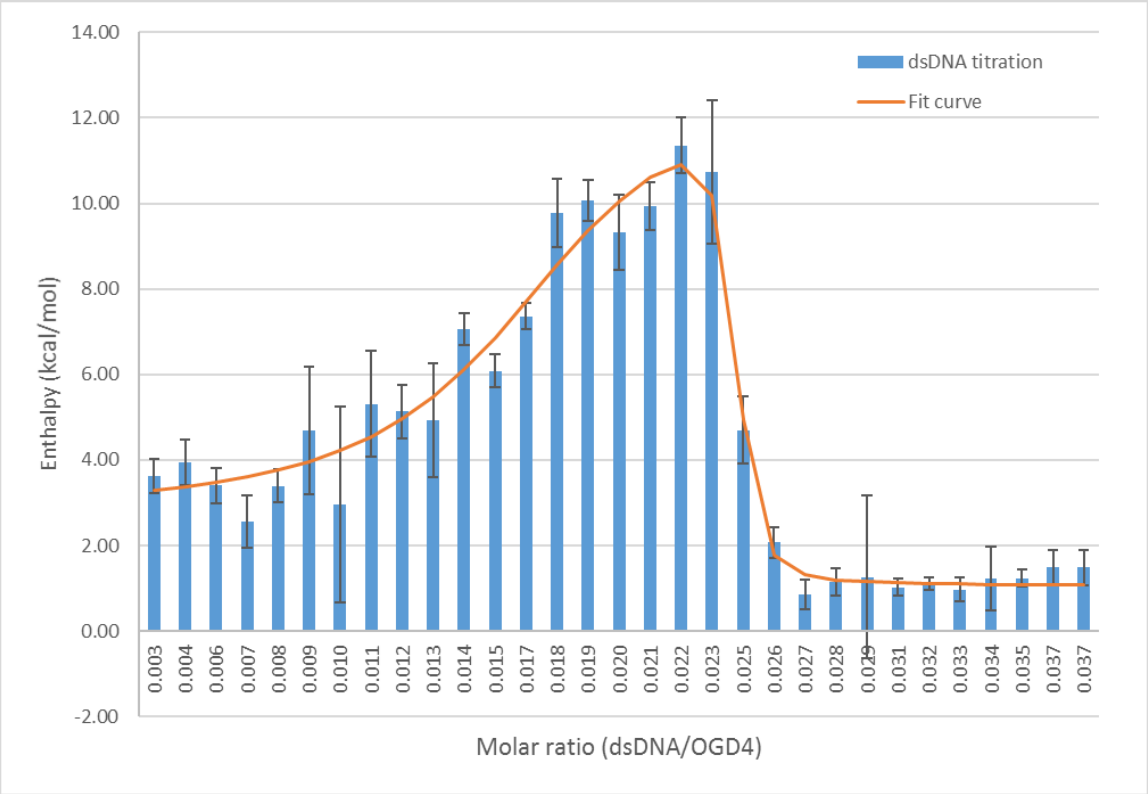

Figure 24. Cumulative heat obtained from the calorimetric titration of 20 µM solution of dsDNA (8 µL/injection) into cationic liposomes that contained 108 µM of OGD4. The figure shows the reaction enthalpy versus the dsDNA/OGD4 molar ratio (blue bars) and the fitted curve (orange line) to obtain the thermodynamic parameters for the interaction.

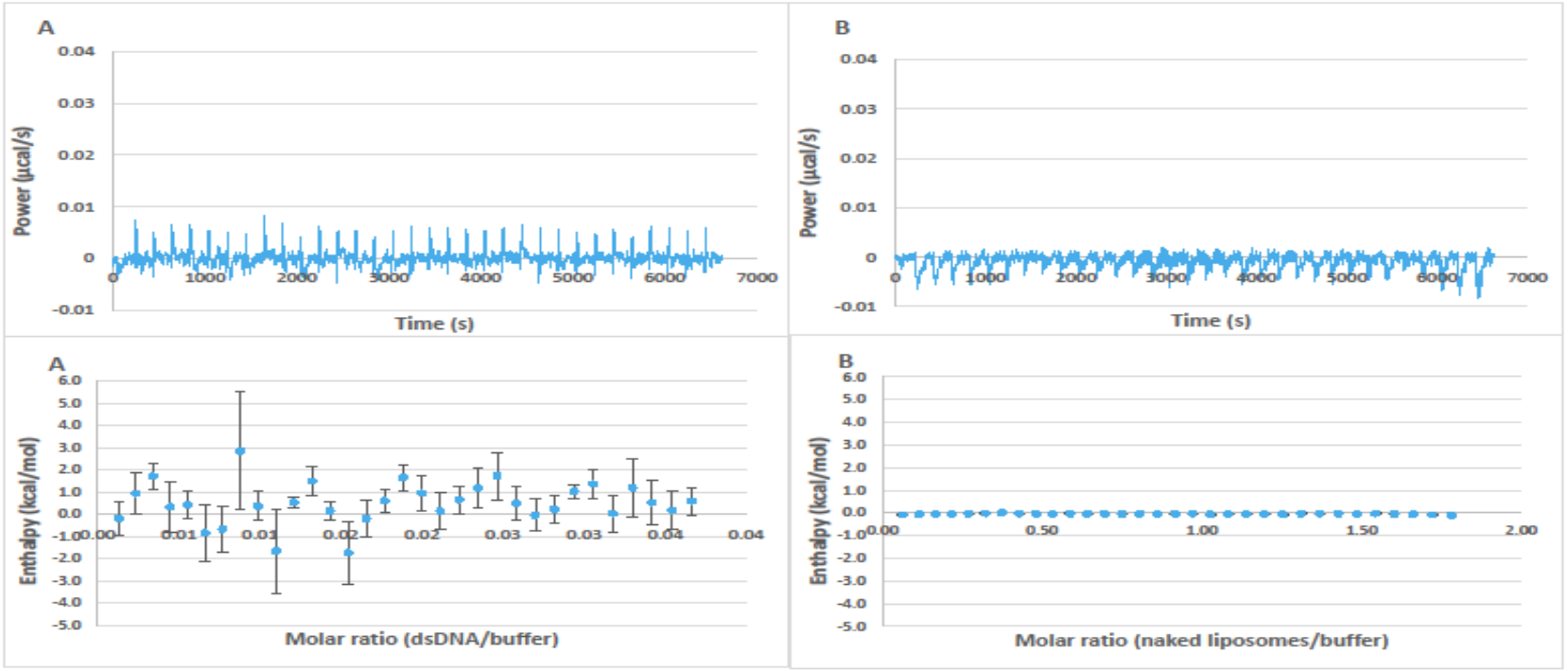

Figure 25. The ITC profiles of (A) dsDNA and (B) naked liposomes titrated into a buffer solution. The upper panels show the raw data and the lower panels show the binding enthalpy of each titration. The concentrations for dsDNA and naked liposomes were 0.02 mM and 0.97 mM, respectively.

The thermodynamic parameters of the dsDNA titration into the cationic liposomes were determined by fitting the ITC data to a chemical interaction model with 2 set of sites. The global parameters Q_{dil} and r_M were also fitted to get these results. The parameters are shown in Table 3. Q_{dil} corrects the molar enthalpy of dilution of the injected solution when control titration has not been subtracted from the experimental data. r_M corrects the possible differences between nominal and true concentration of lipids. The concentration difference may be the result of using the OGD4 concentration instead of the total liposome concentration in the cell. The χ^2 (chi square) value represents the quality of the fit. The cationic liposomes have a high positive charge and are surrounded by the counter ions of the buffer, before the dsDNA replaces them. Each set of fit parameters consists of a binding constant K_a, a stoichiometry parameter N, and a molar enthalpy change ΔH. By using the fitted parameters, we may calculate other quantities describing the reaction: the dissociation constant

$$K_d = \frac{1}{K_a} \tag{11}$$

of the reaction, the molar Gibbs free energy change

$$\Delta G = RT \ln K_d, \tag{12}$$

where R is the gas constant and T the absolute temperature, and the molar reaction entropy

$$\Delta S = \frac{\Delta H - \Delta G}{T}. \tag{13}$$

We expect the first set of parameters to describe the dsDNA/OGD4 reaction. N_1 is roughly the phosphorous/nitrogenous (P/N) ratio of OGD4 and dsDNA at the saturation point. Since ΔH_1 was positive and ΔG_1 was negative, the reaction was endothermic and spontaneous, respectively (Sinko and Singh 2011b). The molar entropy change ΔS_1 is due to the movement of the counter ions during the dsDNA binding to OGD4 (Ziegler and Seelig 2007). The reaction was entropy driven because the molar enthalpy change ΔH_1 was smaller than $T\Delta S_1$ (24400 cal/mol) (Bouchemal and Mazzaferro 2012; Wettig andKamel 2013). The second set of parameters is responsible for the drop in the heat curve in Figure 24, and should correspond to a secondary reaction (e.g. aggregation).

The enthalpy reaches its maximum when the maximal amount of dsDNA is bound to the cationic liposomes. The N/P ratio at the maximum was calculated from the dsDNA and

OGD4 concentrations using Equation 10 and was found to be 4.4. The calculations are included in APPENDIX A: . Towards the end of the titration when the enthalpy change was again low, no more dsDNA could bind to the cationic liposomes and any additional dsDNA remained free in the solution.

Table 3. Fitting parameters for the ITC enthalpy curve: reaction stoichiometry N, affinity constant K_a and molar enthalpy change ΔH. Additionally two global fitting parameters were used: the molar enthalpy of dilution Q_{dil} and the lipid concentration correction coefficient r_M. The dissociation constant K_d, molar reaction entropy ΔS, and molar Gibbs free energy change ΔG were computed from the fitted parameters as explained in the text.

Set one parameters			Set two parameters		
N_1	0.23	± 0.01	N_2	0.46	± 0.02
K_{a1} (L/mol)	7.3×10^{8}	± 8.6×10^{7}	K_{a2} (L/mol)	9.3×10^{9}	± 3.7×10^{9}
K_{d1} (mol/L)	1.4×10^{-9}		K_{d2} (mol/L)	1.1×10^{-10}	
ΔH_1 (cal/mol)	12300	± 536	ΔH_2 (cal/mol)	1450	± 165
ΔS_1 (cal/(K mol))	81.9		ΔS_2 (cal/(K mol))	50.4	
ΔG_1 (cal/mol)	-12100		ΔG_2 (cal/mol)	-13600	
Q_{dil} (cal/mol)	1300	± 12	r_M	0.034	± 9.0×10^{-4}
Quality of the fit	$\chi 2$	1.01			

5.4 Dynamic light scattering results for OGD6

The characterization of the OGD6 was also started by measuring the size and zeta potential of liposomes that contained different amounts of OGD6. These measurements were performed in HEPES (pH 7.4) buffer, and the total lipid concentration of the sample was 1 mg/mL. These results are shown in Table 4 and Figure 26. For further studies the mol-% of OGD6 in liposomes was chosen to be 5 %. This was the smallest amount of OGD6 that yielded a sufficiently high zeta potential, and had a reasonably low PDI. The liposome size did not show a strong dependence on the OGD6 percentage.

Table 4. Size and zeta potential measurements, and polydispersity index (PDI) for liposomes with different mol-% of OGD6. The measurements were done in HEPES buffer at pH 7.4 and the total lipid concentration of the sample was 1 mg/mL.

Percentage of OGD6	PDI	Size (nm)	Zeta potential (mV)
0.00 %	0.28	189.24 ±6.00	-3.31 ±1.27
2.50 %	0.24	203.72 ±9.02	7.28 ±0.65
5.00 %	0.21	200.00 ±6.67	15.03 ±0.76
7.50 %	0.19	201.58 ±4.98	18.13 ±0.29
10.00 %	0.29	190.24 ±9.43	18.83 ±0.35

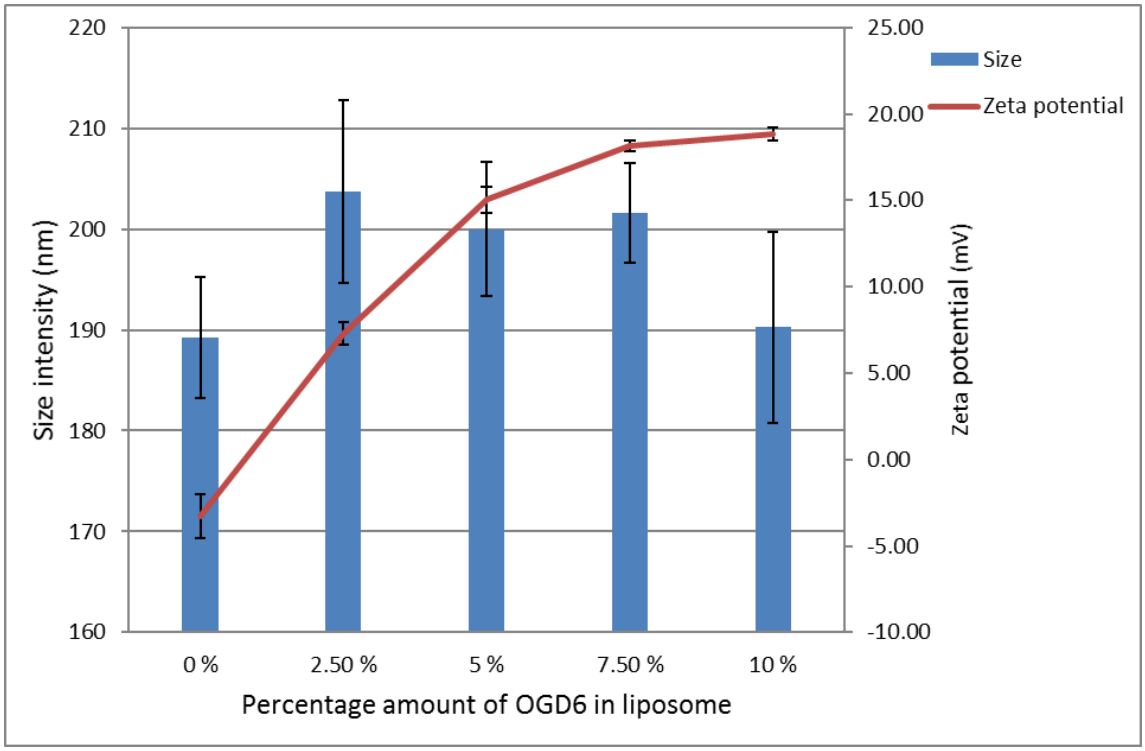

Figure 26. Size and zeta potential for liposomes with different mol-% of OGD6. The buffer was HEPES, and the total lipid concentration of the sample was 1 mg/mL. The bars show the size of the liposomes and the line represents the zeta potential.

Figure 27 shows the size and zeta potential of the cationic OGD6 liposomes that contained different amounts of dsDNA, measured in HEPES (pH 7.4) buffer. Figure 28 represents the corresponding size and zeta potential measurements in citrate buffer at pH 5. Figure 29 shows the PDI values for the size results of OGD6 lipoplexes. The N/P ratio describes the relation between the positive charge from the OGD6 and the negative charge from the dsDNA. It can be seen in Figure 27 that all the positive charges are compensated when

the N/P ratio is between 1–2.5 in HEPES (pH 7.4) buffer, as this is where the zeta potential reaches zero.

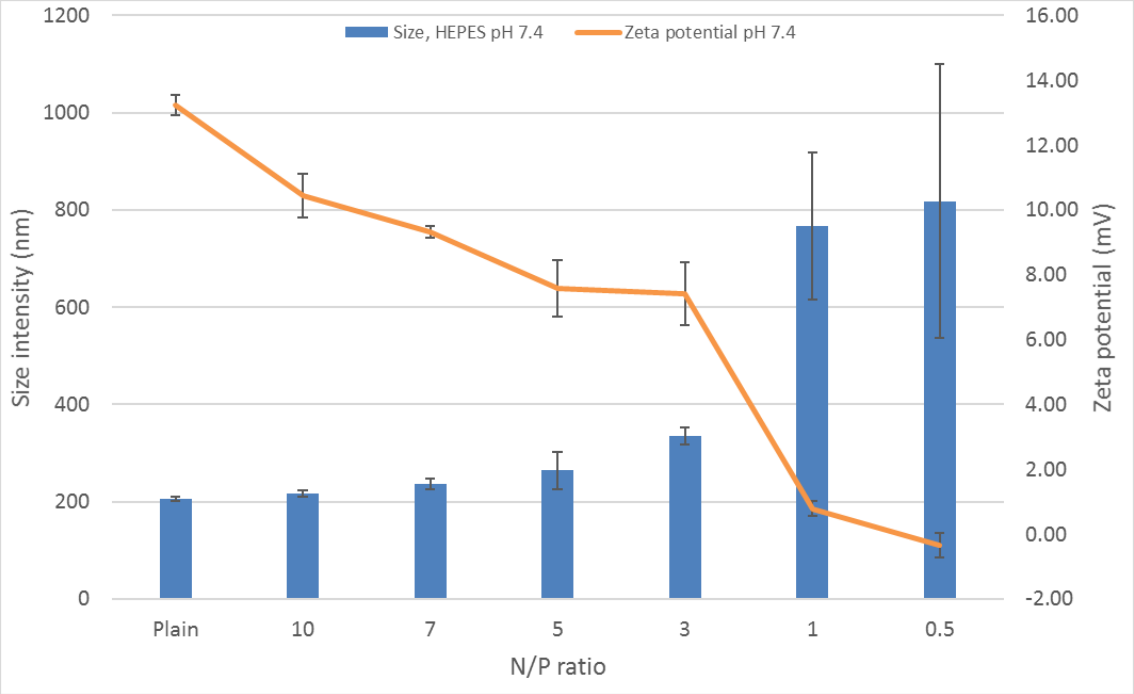

Figure 27. Size and zeta potential of the lipoplexes in HEPES buffer at pH 7.4 as a function of the N/P ratio, with a total lipid concentration of 0.1 mg/mL. The amount of dsDNA is increasing as the N/P ratio decreases. The plain liposomes do not contain any dsDNA. The bars show the size of the lipoplexes and the line represents the zeta potential.

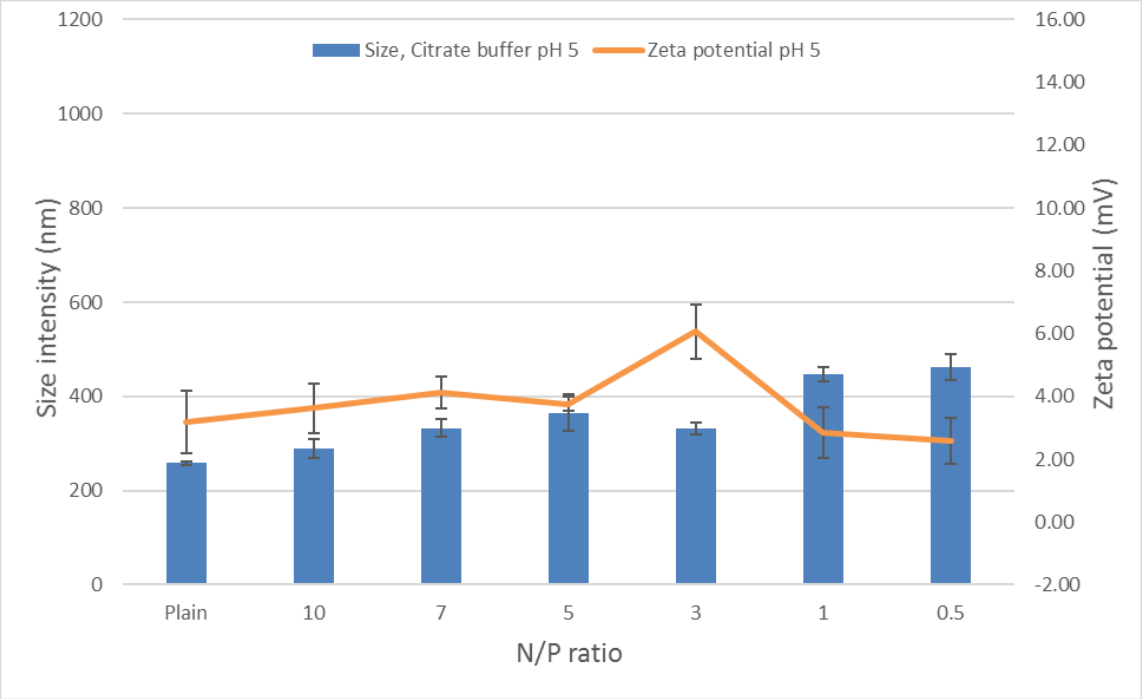

Figure 28. Size and zeta potential of the lipoplexes in citrate buffer at pH 5 as a function of the N/P ratio, with a total lipid concentration of 0.1 mg/mL. The amount of dsDNA is increasing as the N/P ratio decreases. The plain liposomes do not contain any dsDNA. The bars show the size of the lipoplexes and the line represents the zeta potential.

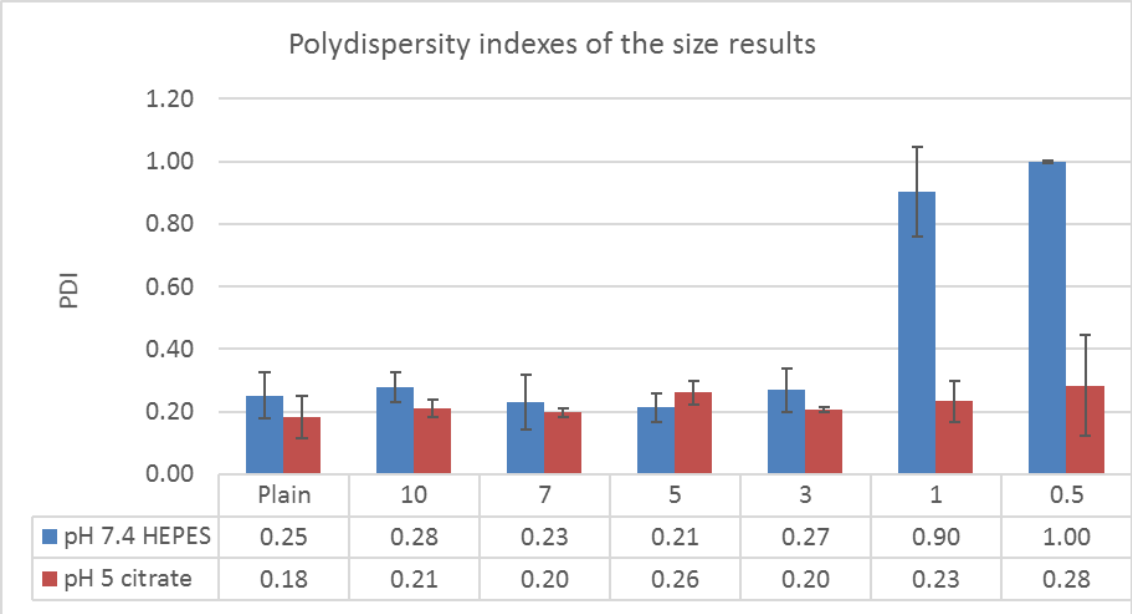

	Plain	10	7	5	3	1	0.5
pH 7.4 HEPES	0.25	0.28	0.23	0.21	0.27	0.90	1.00
pH 5 citrate	0.18	0.21	0.20	0.26	0.20	0.23	0.28

Figure 29. The polydispersity index of the ODG6 size results. Each N/P ratio has the PDI results for lipoplexes in HEPES buffer at pH 7.4 (blue bars), and citrate buffer at pH 5 (red bars). The total lipid concentration of the sample was 0.1 mg/mL. The amount of the dsDNA is increasing as the N/P ratio decreases. The plain liposomes do not contain any dsDNA.

5.5 Electrophoretic mobility shift assay for OGD6

Two electrophoretic mobility shift assays were also performed for OGD6 liposomes. One (gel A) at pH 7.4 using the TBE buffer to run the electrophoresis, and the other (gel B) at pH 5.0 using 80 mM citrate buffer. The liposomes were prepared in 10 mM HEPES buffer (pH 7.4) or 80 mM citrate buffer (pH 5.0), respectively. Figure 30 shows the electrophoretic profiles of the gels. At pH 7.4 one can see that there was some free dsDNA remaining when the N/P ratio was smaller than 1, and all the dsDNA was attached to the OGD on the liposome surface when the N/P ratio was 3 or greater. At pH 5 the profile is the same as at pH 7.4. This means that the pH does not significantly affect how the OGD6 liposomes can complex dsDNA.

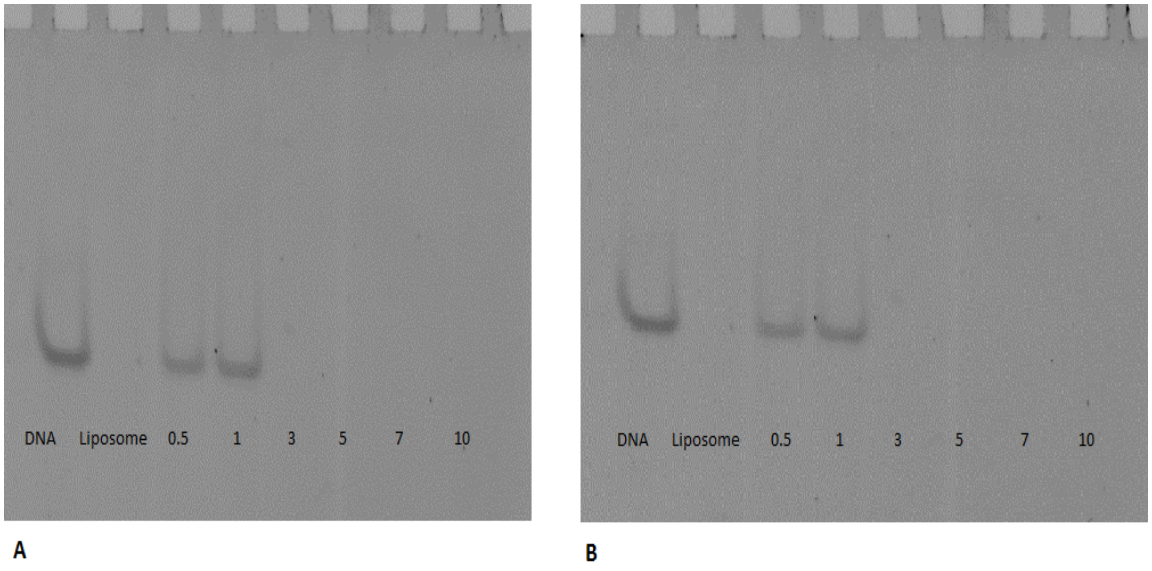

Figure 30. Electrophoretic mobility profiles of dsDNA mixed with OGD6 liposomes (A) at pH 7.4 and (B) at pH 5.

6 DISCUSSION

6.1 Characterization studies

The focus of the characterization studies was to obtain the optimal cationic liposome composition for associating dsDNA in order to form a novel lipoplex for gene delivery.

Most of the characterization studies were performed on OGD4 liposomes because there were difficulties in synthetizing a sufficient amount of OGD6 lipids to perform all the planned studies. The characterization involved two steps: determining the optimal amount of OGD in the liposome, and then determining how much dsDNA can be associated with it.

The hydrodynamic size of the particles was measured by DLS. According to the PDI values, both the OGD4 cationic liposomes and lipoplexes are either moderately (PDI 0.1–0.4) or highly (PDI > 0.4) polydisperse (Bhattacharjee 2016), as can be seen in Figure 16,Figure 17 andFigure 18. Based on the zeta potential measurement 10 % of OGD4 was used in the liposome composition. For lipoplexes the HEPES buffer resulted in the most consistent size and the lowest PDI (around 0.2), while the TRIS and citrate buffers yielded lipoplexes with a greater PDI and a size that varied more. Furthermore, the PDI of the citrate buffer lipoplexes was around 1 which means that the size measurement was unreliable and would need to be repeated to get adequate results, perhaps by using another method. The TRIS buffer lipoplexes were also quite polydisperse with a PDI around 0.5. The lipoplex zeta potential decreased to zero around an N/P ratio of 5 for HEPES and around an N/P ratio of 1 for TRIS.

Figure 27Figure 28 andFigure 29 show the size measurement results and PDIs of OGD6 liposomes and lipoplexes. The OGD6 liposomes had an overall lower PDI than the OGD4 liposomes. Based on the zeta potential measurements, the optimal liposome composition was chosen to include 5 % of OGD6. In HEPES buffer at pH 7.4 a simultaneous decrease in the zeta potential and an increase in size and PDI around the N/P ratio 1 were seen, which may be related to the positive charges being compeletely compensated. In the pH 5 citrate buffer no such transition could be seen, and the zeta potential never reached over +6 mV.

The size and zeta potential measurements were performed in three different buffers (HEPES, TRIS and citrate). The salt concentration of HEPES and citrate buffers were adjusted to create an isotonic osmotic pressure. The salt concentration for TRIS buffer was smaller than for HEPES or citrate buffers, and therefore the ionic strength and

osmotic pressure were also smaller as shown in Table 1. The ionic strength of the citrate buffer was 0.480 which was much larger than that of HEPES (0.160) and TRIS (0.068). The ionic strength can affect the zeta potential results and therefore the zeta potential results of citrate buffer lipoplexes should be used in a relative, not absolute sense (Kaszuba et al. 2010). The zeta potential results of OGD4 lipoplexes (Figure 19) showed that more dsDNA is needed to compensate the cationic charges of ODG4 liposomes when they are in a lower ionic strength (TRIS) buffer. This is due to the increase of the electrostatic interaction between the oppositely charged components of the complex (Kennedy et al. 2000).

The electrophoretic mobility shift assay was performed by using the APS-TEMED system as the initiator to prepare the polyacrylamide gel. The APS-TEMED systems has an optimal polymerization performance when the pH is 7–10, and no polymerization at pH 4 (Caglio and Righetti 1993). With OGD4 in the citrate buffer the gel formation (at pH 5) was weak, and the resulting gel was more fluid than at pH 7.4. The methylene blue system could perform better at low pH (Caglio and Righetti 1993). By comparing the electrophoresis results it can be seen that OGD4 lipoplexes were more pH dependent than OGD6 lipoplexes. At pH 5 OGD4 lipoplexes needed more dsDNA to compensate all the cationic charges than at pH 7.4, whereas OGD6 lipoplexes could bind the same amount of dsDNA at both pH values.

The thermodynamic properties of dsDNA binding to the OGD4 liposomes were obtained by ITC. The fitted parameters are presented in Table 3. The large first binding constant indicates that the interaction between the dsDNA and OGD4 is electrostatic and strong. Similar observations were made by Nascimento et al. (2015) when they studied the interaction between cationic liposomes and siRNA by ITC. The binding reaction in this study was endothermic (ΔH_1 is 12300 ± 536 cal/mol) and entropy driven, as was also found in previous ITC experiments involving cationic liposomes and DNA (Kennedy et al. 2000; Pozharski and MacDonald 2002; Lobo et al. 2003). The global Q_{dil} parameter (1300 ± 12 cal/mol) denoting the molar dilution enthalpy was compatible with the control titration in Figure 25 A. After the saturation point of the reaction the electrostatic interactions and hydrogen bonds weaken and therefore the molar enthalpy change

decreases from 12300 to 1450 cal/mol. This can be explained by aggregation of the OGD4 lipoplexes after the surface charge of the lipoplex becomes neutral (Kennedy et al. 2000). This explanation is also supported by the results in Figure 17 Figure 19 where the size of the TRIS buffer lipoplexes increased three times as the zeta potential approached zero around N/P ratio 1, respectively. The same phenomenon could also be seen with OGD6 in HEPES buffer in Figure 27.

All characterization studies were completed with the combination of OGD4 lipoplexes in TRIS buffer. The electrophoresis gel A in Figure 22 shows that below an N/P ratio of 5 there is some free dsDNA left, and the ITC study yielded the compatible equilibrium N/P ratio of 4.4. Around N/P ratio 2 the lipoplex size started to increase, and the zeta potential decreased to zero around N/P ratio 1. Therefore, it seems that the optimal N/P ratio for the lipoplexes is around 5.

6.2 Future perspectives

In this study, we investigated the characteristics of the novel oligo-guanidyl cationic lipoplex developed for gene delivery. Since a high ionic strength distorts the zeta potential results, the zeta potential studies should be repeated using HEPES buffer without sodium chloride and the citrate buffer at pH 5 should be replaced with another suitable buffer for the corresponding pH in order to obtain more reliable results. Also, the electrophoretic mobility shift assay at pH 5 should be repeated using the methylene blue system instead of APS-TEMED (Caglio and Righetti 1993). More complete ITC results could be obtained by repeating the titration a few times in both directions (dsDNA into OGD4 liposomes and vice versa). The complete characterization of OGD6 lipoplexes also remains to be done.

Instead of the post insertion method, another way to produce the cationic liposomes is to mix the OGD lipid together with EggPC and cholesterol stock solutions in the round bottom flask and prepare a thin lipid film containing both the neutral lipids and the cationic OGD lipid. Then the lipid film is rehydrated with dsDNA solution prior the ten freeze-thaw cycles, sonication, and extrusion. The lipoplexes prepared in this way should

be compared and contrasted with the lipoplexes prepared by post-insertion method in order to determine the best approach to prepare the lipoplexes for *in vitro* and *in vivo* studies. Also, a DNA release study remains to be performed on both types of lipoplexes.

For further investigations, e.g. release or cell studies with OGD4 lipoplexes with an N/P ratio of 4.4−5 are recommended because charge neutral lipoplexes aggregate easier and reduce the gene expression (Tros de Ilarduya et al. 2010). Also, for optimized stability the lipoplex surface should be slightly positive. In *in vitro* and *in vivo* studies it is important to avoid rapid elimination by RES e.g. by coating the liposomes with PEG (Nayerossadat et al. 2012). It would also be interesting to determine how the dsDNA is associated to the OGD and to the liposome, e.g. whether the dsDNA is encapsulated inside the cationic liposome or resides on the liposome surface. These morphological characteristics could be determined by using imaging techniques such as Transmission Electron Microscopy.

7 CONCLUSION

The focus of this study was to develop and characterize a novel poly-cationic liposomal platform for gene delivery. The novel synthetic non-peptide oligo-guanidyl derivative (OGD) was post inserted into the lipid bilayer and then characterized to obtain a liposome formulation that contains the smallest amount of OGD that results in sufficiently high zeta potential and uniform, sufficiently small size. The optimal formulation contained either 10 % of OGD4 or 5 % of OGD6 of the total lipid amount. The second step of the characterization studies was to find the smallest N/P ratio (the highest dsDNA loading) at which most of the cationic molecules were associated with dsDNA but a small positive charge remained on the lipoplex surface. DLS studies for OGD4 and OGD6 lipoplexes were performed in isotonic buffers, HEPES (pH 7.4) and citrate (pH 5) to mimic the conditions in human blood and cell endosome, respectively. The electrophoresis studies for both types of lipoplexes were performed in TBE (pH 7.4) and citrate buffers because TBE was used as the gel running buffer at pH 7.4. The ITC measurements were performed in non-isotonic TRIS buffer because it has a lower ionic strength than the isotonic HEPES

buffer, and TRIS was also used as annealing buffer for dsDNA. To obtain complete results for OGD4 lipoplexes, also the DLS, zeta potential and electrophoresis studies were performed in TRIS buffer. For further investigations, e.g. release or cell studies, the optimal OGD4 lipoplexes were determined to have an N/P ratio of around 5. Further investigations would be needed to determine the best lipoplex composition and manufacturing method using an isotonic buffer in all the measurements excluding the zeta potential since the zeta potential results are not reliable when the ionic strength of the sample is high.

BIBLIOGRAPHY

Akbarzadeh A, Rezaei-Sadabady R, Davaran S et al.: Liposome: classification, preparation, and applications (online). Springer Open, 2013 (referred to 3 March 2017). Available: http://www.nanoscalereslett.com/content/8/1/102

Alhakamy NA, Nigatu AS, Berkland CJ, Ramsey JD: Noncovalently associated cell-penetrating peptides for gene delivery applications. Ther Deliv 4: 741-757, 2013

Allen TM, Cullis PR: Liposomal drug delivery systems: From concept to clinical applications. Adv Drug Deliv Rev 65: 36-48, 2013

Avanti Lipids Polar I: Avanti Polar Lipids, Inc. Product. Hydro Soy PC.October. Available: https://avantilipids.com/product/840058/

Bangham AD, Standish MM, Watkins JC: Diffusion of univalent ions across the lamellae of swollen phospholipids. J Mol Biol 13: 238-252, 1965

Bersani Sara, Salmaso Stefano, Mastrotto Francesca, Ravazzolo Elena, Semenzato Alessandra, Caliceti Paolo: Star-Like Oligo-Arginyl-Maltotriosyl Derivatives as Novel Cell-Penetrating Enhancers for the Intracellular Delivery of Colloidal Therapeutic Systems. Bioconjug Chem 23: 1415-1425, 2012

Bhattacharjee S: DLS and zeta potential – What they are and what they are not? J Controlled Release 235: 337-351, 2016

Bouchemal K, Mazzaferro S: How to conduct and interpret ITC experiments accurately for cyclodextrin–guest interactions. Drug Discov Today 17: 623-629, 2012

Brookhaven Instruments: NanoDLS: Particle Size Analyzer for Flow & Batch Mode Applications October. Available: http://www.brookhaveninstruments.com/nanodls

Caglio S, Righetti PG: On the pH dependence of polymerization efficiency, as investigated by capillary zone electrophoresis. Electrophoresis 14: 554-558, 1993

Cardarelli F, Digiacomo L, Marchini C et al.: The intracellular trafficking mechanism of Lipofectamine-based transfection reagents and its implication for gene delivery. Sci Rep 6: 2016

Castile JD, Taylor KMG: Factors affecting the size distribution of liposomes produced by freeze–thaw extrusion. Int J Pharm 188: 87-95, 1999

Dalby B, Cates S, Harris A et al.: Advanced transfection with Lipofectamine 2000 reagent: primary neurons, siRNA, and high-throughput applications. Methods 33: 95-103, 2004

Drabik A, Bodzon-Kulakowska A, Silberring J: 6 - Gel Electrophoresis. In:Proteomic Profiling and Analytical Chemistry, pp. 107-133, Ed. Ciborowski P, Silberring J, Elsevier, Amsterdam 2013

Fan Y, Zhang Q: Development of liposomal formulations: From concept to clinical investigations. Asian Journal of Pharmaceutical Science 8: 81-87, 2013

Fischer K, Schmidt M: Pitfalls and novel applications of particle sizing by dynamic light scattering. Biomaterials 98: 79-91, 2016

Frankel AD, Pabo CO: Cellular uptake of the tat protein from human immunodeficiency virus. Cell 55: 1189-1193, 1988

Frézard F, Silva-Barcellos NM, dos Santos RAS: A novel approach based on nanotechnology for investigating the chronic actions of short-lived peptides in specific sites of the brain. Regul Pept 138: 59-65, 2007

Gabizon AA: Stealth Liposomes and Tumor Targeting: One Step Further in the Quest for the Magic Bullet. Clin Cancer RES 7: 223-225, 2001

Gaumet M, Vargas A, Gurny R, Delie F: Nanoparticles for drug delivery: the need for precision in reporting particle size parameters. Eur J Pharm Biopharm 69: 1-9, 2008

Geoghegan JC, Gilmore BL, Davidson BL: Gene Silencing Mediated by siRNA-binding Fusion Proteins Is Attenuated by Double-stranded RNA-binding Domain Structure. Mol Ther Nucleic Acids 1: e53, 2012

Gregoriadis G: Drug entrapment in liposomes. FEBS Lett 36: 292-296, 1973

Herce HD, Garcia AE: Cell penetrating peptides: How do they do it? J Biol Phys 33: 345-356, 2007

Herce HD, Garcia AE, Cardoso CM: Fundamental molecular mechanism for the cellular uptake of guanidinium-rich molecules. J Am Chem Soc 136: 17459-17467, 2014

International Organization for Standardization: Particle size analysis — Dynamic light scattering (DLS). ISO 22 412. edition. Anonymous ISO, Geneva, Switzerland 2008

Järver P, Langel U: Cell-penetrating peptides--a brief introduction. Biochim Biophys Acta 1758: 260-263, 2006

Kaszuba M, Corbett J, Watson FM, Jones A: High-concentration zeta potential measurements using light-scattering techniques. Philos Trans A Math Phys Eng Sci 368: 4439-4451, 2010

Kennedy MT, Pozharski EV, Rakhmanova VA, MacDonald RC: Factors Governing the Assembly of Cationic Phospholipid-DNA Complexes. Biophys J 78: 1620-1633, 2000

Kerek EM, Prenner EJ: Inorganic cadmium affects the fluidity and size of phospholipid based liposomes. Biochim Biophys Acta 1858: 3169-3181, 2016

Koide H, Okamoto A, Tsuchida H et al.: One-step encapsulation of siRNA between lipid-layers of multi-layer polycation liposomes by lipoplex freeze-thawing. J Controlled Release 228: 1-8, 2016

Li J, Wang X, Zhang T et al.: A review on phospholipids and their main applications in drug delivery systems. Asian Journal of Pharmaceutical Sciences 10: 81-98, 2015

Lipoid GmbH: Lipoid: Phosphatidylcholine October. Available: http://www.lipoid.com/en/phosphatidylcholine

Lobo BA, Koe GS, Koe JG, Middaugh CR: Thermodynamic analysis of binding and protonation in DOTAP/DOPE (1:1): DNA complexes using isothermal titration calorimetry. Biophys Chem 104: 67-78, 2003

Lopes Sávia, Giuberti Cristiane, Rocha Talita, Ferreira Diego, Leite Elaine, Oliveira Mônica: Liposomes as Carriers of Anticancer Drugs. In: Cancer Treatment - Conventional and Innovative Approaches, pp. 85-124, Ed. Rangel L, InTech, 2013

NanoComposix: NanoComposix's guíde to dynamic light scattering measurement and analysis. 1.4: 2015.

Nascimento Thais L., Hillaireau Hervé, Noiray Magali et al.: Supramolecular Organization and siRNA Binding of Hyaluronic Acid-Coated Lipoplexes for Targeted Delivery to the CD44 Receptor. Langmuir 31: 11186-11194, 2015

Nayerossadat N, Maedeh T, Ali PA: Viral and nonviral delivery systems for gene delivery.(Review Article)(Report). Adv Biomed Res 1: 27, 2012

Pierce MM, Raman CS, Nall BT: Isothermal titration calorimetry of protein-protein interactions. Methods 19: 213-221, 1999

Pozharski E, MacDonald RC: Thermodynamics of cationic lipid-DNA complex formation as studied by isothermal titration calorimetry. Biophys J 83: 556-565, 2002

Rasoulianboroujeni M, Kupgan G, Moghadam F et al.: Development of a DNA-liposome complex for gene delivery applications. Materials Science and Engineering: C 75: 191-197, 2017

Sebaaly C, Greige-Gerges H, Stainmesse S, Fessi H, Charcosset C: Effect of composition, hydrogenation of phospholipids and lyophilization on the characteristics of eugenol-loaded liposomes prepared by ethanol injection method. Food Bioscience 15: 1-10, 2016

Shi Q, Jackowski G: One-dimensional polyacrylamide gel electrophoresis. In:Gel Electrophoresis of Proteins : A Practical Approach, pp. 1-52, Ed. Hames BD, OUP Oxford, Oxford 1998

Sigma-Aldrich: Products: Cholesterol October. Available: http://www.sigmaaldrich.com/catalog/product/sigma/c8667?lang=fi&region=FI

Sinko PJ, Singh Y: Chapter 13: Drug release and dissolution. In:Martin's physical pharmacy and pharmaceutical sciences : physical chemical and biopharmaceutical principles in the pharmaceutical sciences, pp. 300-317, 6th ed. edition. Anonymous Lippincott Williams & Wilkins, Philadelphia 2011

Sinko PJ, Singh Y: Chapter 3: Thermodynamics. In:Martin's physical pharmacy and pharmaceutical sciences : physical chemical and biopharmaceutical principles in the pharmaceutical sciences, pp. 54-76, 6th ed. edition. Anonymous Lippincott Williams & Wilkins, Philadelphia 2011

Sinko PJ, Singh Y: Chapter 6: Electrolyte solutions. In:Martin's physical pharmacy and pharmaceutical sciences : physical chemical and biopharmaceutical principles in the pharmaceutical sciences, pp. 129-145, 6th ed. edition. Anonymous Lippincott Williams & Wilkins, Philadelphia 2011

Sorkin A, von Zastrow M: Signal transduction and endocytosis: close encounters of many kinds. Nature Reviews Molecular Cell Biology 3: 600-614, 2002

Stiufiuc R, Iacovita C, Stiufiuc G, Florea A, Achim M, Lucaciu CM: A new class of pegylated plasmonic liposomes: Synthesis and characterization. J Colloid Interface Sci 437: 17-23, 2015

Technical note: Dynamic Light Scattering: An Introduction in 30 Minutes October. Available online:http://www.malvern.com/en/support/resource-center/technical-notes/TN101104DynamicLightScatteringIntroduction.aspx

Torchilin VP, Rammohan R, Weissig V, Levchenko TS: TAT peptide on the surface of liposomes affords their efficient intracellular delivery even at low temperature and in the presence of metabolic inhibitors. Proc Natl Acad Sci U S A 98: 8786-8791, 2001

Tros de Ilarduya C, Sun Y, Düzgüneş N: Gene delivery by lipoplexes and polyplexes. Eur J Pharm Sci 40: 159-170, 2010

Uskokovic V, Castiglione Z, Cubas P, Zhu L, Li W, Habelitz S: Zeta-potential and particle size analysis of human amelogenins. J Dent Res 89: 149-153, 2010

Varenne F, Botton J, Merlet C, Beck-Broichsitter M, Legrand F, Vauthier C: Standardization and validation of a protocol of size measurements by dynamic light scattering for monodispersed stable nanomaterial characterization. Colloids and Surfaces A: Physicochemical and Engineering Aspects 486: 124-138, 2015

Varga Z, Yuana Y, Grootemaat AE et al.: Towards traceable size determination of extracellular vesicles (online). Journal of Extracellular Vesicles, 2014 (referred to February 4th). Available: http://dx.doi.org/10.3402/jev.v3.23298

Wettig Shawn D., andKamel Amany O.: Thermodynamic Studies of DNA-Cationic Components Interactions Using Titration Calorimetry. J Thermodyn Catal 4: 121-126, 2013

Zuo T, Guan Y, Chang M et al.: RGD(Arg-Gly-Asp) internalized docetaxel-loaded pH sensitive liposomes: Preparation, characterization and antitumor efficacy in vivo and in vitro. Colloids Surf B Biointerfaces 147: 90-99, 2016

APPENDIX A: Isothermal titration calorimetry raw data

	OGD4 liposomes in the cell						dsDNA in the syringe							
Injection number	Initial volume (mL)	Injected volume (mL)	Final volume (L)	Initial concentration in cell (mM)	Final concentration in cell (mM)	Final amount of OGD4 (mmol)	Final volume in cell (L)	Injected volume (mL)	Final volume in syringe (mL)	Final concentration in cell (mM)	Final amount in cell (mmol)	N/P ratio in cell	dsDNA/ OGD4 molar ratio	P/N ratio in cell
0	1.42	0	1.42E-03	0.1080	0.1080	1.54E-04	0	0	0.2796	0.00E+00	0	0	0.000	0.000
1	1.42	0.002	1.42E-03	0.1080	0.1078	1.54E-04	2.00E-06	0.002	0.2776	2.81E-05	4.00E-08	404.09	0.000	0.002
2	1.42	0.008	1.43E-03	0.1078	0.1074	1.54E-04	1.00E-05	0.008	0.2696	1.40E-04	2.00E-07	80.82	0.001	0.012
3	1.42	0.008	1.43E-03	0.1074	0.1074	1.54E-04	1.80E-05	0.008	0.2616	2.52E-04	3.60E-07	44.90	0.002	0.022
4	1.42	0.008	1.43E-03	0.1074	0.1074	1.54E-04	2.60E-05	0.008	0.2536	3.64E-04	5.20E-07	31.08	0.003	0.032
5	1.42	0.008	1.43E-03	0.1074	0.1074	1.54E-04	3.40E-05	0.008	0.2456	4.76E-04	6.80E-07	23.77	0.004	0.042
6	1.42	0.008	1.43E-03	0.1074	0.1074	1.54E-04	4.20E-05	0.008	0.2376	5.87E-04	8.40E-07	19.24	0.005	0.052
7	1.42	0.008	1.43E-03	0.1074	0.1074	1.54E-04	5.00E-05	0.008	0.2296	6.99E-04	1.00E-06	16.16	0.007	0.062
8	1.42	0.008	1.43E-03	0.1074	0.1074	1.54E-04	5.80E-05	0.008	0.2216	8.11E-04	1.16E-06	13.93	0.008	0.072
9	1.42	0.008	1.43E-03	0.1074	0.1074	1.54E-04	6.60E-05	0.008	0.2136	9.23E-04	1.32E-06	12.25	0.009	0.082
10	1.42	0.008	1.43E-03	0.1074	0.1074	1.54E-04	7.40E-05	0.008	0.2056	1.04E-03	1.48E-06	10.92	0.010	0.092
11	1.42	0.008	1.43E-03	0.1074	0.1074	1.54E-04	8.20E-05	0.008	0.1976	1.15E-03	1.64E-06	9.86	0.011	0.101
12	1.42	0.008	1.43E-03	0.1074	0.1074	1.54E-04	9.00E-05	0.008	0.1896	1.26E-03	1.80E-06	8.98	0.012	0.111
13	1.42	0.008	1.43E-03	0.1074	0.1074	1.54E-04	9.80E-05	0.008	0.1816	1.37E-03	1.96E-06	8.25	0.013	0.121
14	1.42	0.008	1.43E-03	0.1074	0.1074	1.54E-04	1.06E-04	0.008	0.1736	1.48E-03	2.12E-06	7.62	0.014	0.131
15	1.42	0.008	1.43E-03	0.1074	0.1074	1.54E-04	1.14E-04	0.008	0.1656	1.59E-03	2.28E-06	7.09	0.015	0.141
16	1.42	0.008	1.43E-03	0.1074	0.1074	1.54E-04	1.22E-04	0.008	0.1576	1.71E-03	2.44E-06	6.62	0.016	0.151
17	1.42	0.008	1.43E-03	0.1074	0.1074	1.54E-04	1.30E-04	0.008	0.1496	1.82E-03	2.60E-06	6.22	0.017	0.161
18	1.42	0.008	1.43E-03	0.1074	0.1074	1.54E-04	1.38E-04	0.008	0.1416	1.93E-03	2.76E-06	5.86	0.018	0.171
19	1.42	0.008	1.43E-03	0.1074	0.1074	1.54E-04	1.46E-04	0.008	0.1336	2.04E-03	2.92E-06	5.54	0.019	0.181
20	1.42	0.008	1.43E-03	0.1074	0.1074	1.54E-04	1.54E-04	0.008	0.1256	2.15E-03	3.08E-06	5.25	0.020	0.191
21	1.42	0.008	1.43E-03	0.1074	0.1074	1.54E-04	1.62E-04	0.008	0.1176	2.27E-03	3.24E-06	4.99	0.021	0.200
22	1.42	0.008	1.43E-03	0.1074	0.1074	1.54E-04	1.70E-04	0.008	0.1096	2.38E-03	3.40E-06	4.75	0.022	0.210
23	1.42	0.008	1.43E-03	0.1074	0.1074	1.54E-04	1.78E-04	0.008	0.1016	2.49E-03	3.56E-06	4.54	0.023	0.220
24	1.42	0.008	1.43E-03	0.1074	0.1074	1.54E-04	1.86E-04	0.008	0.0936	2.60E-03	3.72E-06	4.35	0.024	0.230
25	1.42	0.008	1.43E-03	0.1074	0.1074	1.54E-04	1.94E-04	0.008	0.0856	2.71E-03	3.88E-06	4.17	0.025	0.240
26	1.42	0.008	1.43E-03	0.1074	0.1074	1.54E-04	2.02E-04	0.008	0.0776	2.83E-03	4.04E-06	4.00	0.026	0.250
27	1.42	0.008	1.43E-03	0.1074	0.1074	1.54E-04	2.10E-04	0.008	0.0696	2.94E-03	4.20E-06	3.85	0.027	0.260
28	1.42	0.008	1.43E-03	0.1074	0.1074	1.54E-04	2.18E-04	0.008	0.0616	3.05E-03	4.36E-06	3.71	0.028	0.270
29	1.42	0.008	1.43E-03	0.1074	0.1074	1.54E-04	2.26E-04	0.008	0.0536	3.16E-03	4.52E-06	3.58	0.029	0.280
30	1.42	0.008	1.43E-03	0.1074	0.1074	1.54E-04	2.34E-04	0.008	0.0456	3.27E-03	4.68E-06	3.45	0.030	0.290
31	1.42	0.008	1.43E-03	0.1074	0.1074	1.54E-04	2.42E-04	0.008	0.0376	3.39E-03	4.84E-06	3.34	0.032	0.299
32	1.42	0.008	1.43E-03	0.1074	0.1074	1.54E-04	2.50E-04	0.008	0.0296	3.50E-03	5.00E-06	3.23	0.033	0.309
33	1.42	0.008	1.43E-03	0.1074	0.1074	1.54E-04	2.58E-04	0.008	0.0216	3.61E-03	5.16E-06	3.13	0.034	0.319